

The Stable Planetary Geometry of the Exosystems in 2:1 Mean Motion Resonance

Ji Jianghui^{1,2}, Kinoshita Hiroshi³, LIU Lin^{4,2}, Nakai Hiroshi³, LI Guangyu^{1,2}

ABSTRACT

We have numerically explored the stable planetary geometry for the multiple systems involved in a 2:1 mean motion resonance, and herein we mainly concentrate on the study of the HD 82943 system by employing two sets of the orbital parameters (Mayor et al. 2004). In the simulations, we find that all stable orbits are related to the 2:1 commensurability that can help to remain the semi-major axes for two companions almost unaltered over the secular evolution for 10^7 yr, and the apsidal phase-locking between two orbits can further enhance the stability for this system, because the eccentricities are simultaneously preserved to restrain the planets from frequent close encounters. For HD 82943, there exist three possible stable configurations: (1) Type I, only $\theta_1 \approx 0^\circ$, (2) Type II, $\theta_1 \approx \theta_2 \approx \theta_3 \approx 0^\circ$ (aligned case), and (3) Type III, $\theta_1 \approx 180^\circ$, $\theta_2 \approx 0^\circ$, $\theta_3 \approx 180^\circ$ (antialigned case), here the lowest eccentricity-type mean motion resonant arguments are $\theta_1 = \lambda_1 - 2\lambda_2 + \varpi_1$ and $\theta_2 = \lambda_1 - 2\lambda_2 + \varpi_2$, the relative apsidal longitudes $\theta_3 = \varpi_1 - \varpi_2 = \Delta\varpi$ (where $\lambda_{1,2}$ are, respectively, the mean longitudes of the inner and outer planets; $\varpi_{1,2}$ are the longitudes of periapse). And we find that the other 2:1 resonant systems (e.g., GJ 876 or HD 160691) may possess one of three stable orbits in their realistic motions. In addition, we also propose a semi-analytical model to study $e_i - \Delta\varpi$ Hamiltonian contours, which are fairly consistent with direct numerical integrations. With the updated fit, we then examine the dependence of the stability of this system on the relative inclination, the planetary mass ratios, the eccentricities and other orbital parameters: in the non-coplanar cases, we find that stability requires the relative inclination being $\sim 25^\circ$ or less; as to the planetary mass ratio, the stable orbits for HD 82943 requires $\sin i \geq 0.50$ for a fixed value or $m_1/m_2 \leq 2$ where m_2 remains for the

¹Purple Mountain Observatory, Chinese Academy of Sciences, Nanjing 210008, China; jijh@pmo.ac.cn

²National Astronomical Observatory, Chinese Academy of Sciences, Beijing 100012, China

³National Astronomical Observatory, Mitaka, Tokyo 181-8588, Japan; kinoshita@nao.ac.jp

⁴Department of Astronomy, Nanjing University, Nanjing 210093, China; xhliao@nju.edu.cn

varying mass ratio; concerning the eccentricities, the system can be always steady when $0 < e_2 \leq 0.24$ and $0 < e_1 < 0.60$. Moreover, we numerically show that the assumed terrestrial bodies cannot survive near the habitable zones for HD 82943 due to the strong perturbations induced by two resonant companions, but these low-mass planets can be dynamically habitable in the GJ 876 system at ~ 1 AU in the numerical surveys. Finally, we present a brief discussion on the origin of the 2:1 resonance for HD 82943.

Subject headings: methods:N-body simulations — celestial mechanics — planetary systems — stars:individual (HD 82943, GJ 876, HD 160691)

1. Introduction

The discovery of the extrasolar planets is opening a new world beyond our solar system. Ever since 1995, Mayor & Queloz (1995) detected the first extrasolar giant Jupiter–51 Peg, and to date there are more than 100 planetary systems discovered ¹(Marcy, Cochran, & Mayor 2000; Butler et al. 2003) using the radial velocity technique in the surveys of nearby young stars. At the time of writing, a dozen of multiple planet systems—HD 82943, GJ 876, HD 168443, HD 74156, 47 Uma, HD 37124, HD 38529, HD 12661, 55 Cnc, ν And (Fischer et al. 2003), HD 169830 (Mayor et al. 2004) and HD 160691 (Jones et al. 2002) were discovered in recent years and this number is undoubtedly cumulative as the measurements are being carried on. Hence, it is necessary to categorize the discovered multiple planetary systems according to their statistical characteristics (such as the distribution of the planetary masses, semi-major axes, eccentricities and metallicity) (Marcy et al. 2003), then to study the correlation between mass ratio and period ratio (Mazeh & Zucker 2003) and further to improve the understanding of the relationship between the planet occurrence rate and stellar metallicity (Santos et al. 2003; Fischer, Valenti, & Marcy 2004). The other key point is to investigate possible stable configurations for the multiple systems, in which the observations reveal that most of them are typically characterized by mean motion resonance (MMR) and (or) apsidal phase-locking between their orbiting companions (Fischer et al. 2003; Ji et al. 2003a; Lee & Peale 2003), so that one can better understand the full dynamics of these systems. In the present study, we mainly focus our attention on the HD 82943 system.

As of April 4, 2001, the Geneva Extrasolar Planet Search Team ² announced the discov-

¹see also <http://cfa-www.harvard.edu/planets/bibli.html> and <http://exoplanets.org/>

²see <http://obswww.unige.ch/~udry/planet/hd82943syst.html>

ery of the HD 82943 planetary system at an ESO press release, consisting of two Jupiter-like planets orbiting the parent star. Subsequently, Israelian et al. (2001, 2003) reported the discovery of ${}^6\text{Li}$ in the atmosphere of this metal-rich solar-type star and indicated that the presence of ${}^6\text{Li}$ can probably be shown as evidence for a planet or planets having been engulfed by the star HD82943. At first, let us review several stellar features for this star: HD 82943 is a G0 star with $B - V = 0.623$, Hipparcos parallax of 36.42 mas, distance of 27.46 pc, and $[\text{Fe}/\text{H}] = 0.29 \pm 0.02$ (Santos et al. 2001, 2003). The star is aged 2.9 Gyr with the stellar mass of $1.15 M_{\odot}$. Similar to the GJ 876 system (Marcy et al. 2001), which is believed that stability of the planetary system might be sustained by the 2:1 mean-motion resonance (MMR) and apsidal alignment in the semi-major axes (Kinoshita & Nakai 2001; Lee & Peale 2002; Ji, Li, & Liu 2002), the two planets of HD 82943 are now also close to a 2:1 commensurability, with orbital periods 435.1 ± 1.4 and 219.4 ± 0.2 d, and semi-major axes 1.18 and 0.75 AU (Mayor et al. 2004). However, the previous investigations (Goździewski & Maciejewski 2001) of the stability of the HD 82943 system showed that the system given by the earlier best-fit orbital solution was extremely unstable due to the strong interaction of two massive planets with high eccentricities, hence a natural question is that whether the two companions for this system are really in a 2:1 orbital resonance and whether the system is secularly stable with the observed best-fit orbital parameters. Additionally, the stability for HD 82943 places constraints on both planetary masses—if the mass of the outer companion is smaller than that of the inner planet (Hadjidemetriou 2002), a system that harbors two planets moving on elliptic 2:1 resonant periodic orbits will be destabilized as a finale. Nevertheless, the recently updated orbital solutions (Mayor et al. 2004), with more abundant observations as of October 13, 2003, show that the inner planet is a bit more massive than the outer one, thus it is indeed noteworthy to thoroughly reanalyze the observed HD 82943 system, still these mentioned issues of this fascinating system are to arouse our great interests and inspire us to seek after the answers. Consequently, our first goal is to carefully explore the system to fully understand in what kind of likely configurations that two companions may orbit about their host star and if exist, to reveal the dynamical mechanisms to remain the system.

In a viewpoint of celestial mechanics, the former studies are concerned for the dynamical analysis for the global stability of the exosystems (Goździewski & Maciejewski 2001, 2003; Ji et al. 2002; Kiseleva-Eggleton et al. 2002; Barnes & Quinn 2004), the investigations of resonant picture in the phase space (Hadjidemetriou 2002; Ji et al. 2003a; Haghighipour et al. 2003; Callegari Jr., Michtchenko, & Ferraz-Mello 2004) or chaotic behavior (Jiang & Yeh 2004) in these systems, and the existence of Habitable Zones (HZ) for Earth-like planets that supply stable liquid-water environment to cultivate extraterrestrial intelligent beings (Kasting, Whitmore, & Reynolds 1993; Jones & Sleep 2002; Laughlin, Chambers, &

Fischer 2002; Dvorak et al. 2003; Menou & Tabachnik 2003). Other recent works on the 2:1 resonant geometry of the extrasolar planetary systems include those by Hadjidemetriou & Psychoyos (2003), Beauge, Ferraz-Mello, & Michtchenko (2003) and Lee (2004). They studied the presence and location of stable equilibrium solutions or dynamical evolution of such exosystems in more general way. In this work, we revisit the dynamics of the HD 82943 system and outline several possible stable configurations for a system harboring two companions in a 2:1 resonance, and our new findings are that this system can be locked in aligned or antialigned orbital motions, which these results are never presented nor analyzed in other studies. Specifically, at first, we introduce the numerical setup (see §2) for the dynamical simulations. In §3, we make a study of the various planetary configurations for HD 82943 by means of the semi-analytical treatment and direct integrations over long-term orbital evolution. We present the numerical results of HD 82943 by employing two series of the best-fit orbital solutions, and we discover three kinds of stable planetary geometry for this system that all are linked to a 2:1 resonance. Furthermore, we advance a semi-analytical model that can avoid the difficulties in the perturbation expansions for the larger eccentricities and still help to explain the numerical evolutions. Still, we investigate how the stability for the resonant topology depends on the planetary mass ratio and the orbital parameters on the basis of the new fit (Mayor et al. 2004). In §4, we explore whether there exist an Earth-like planet surviving about the Habitable zones for the authentic systems of HD 82943 and GJ 876.

The other extraordinary phenomenon in the exosystems is that many of them can host giant Jupiter-like planets with strikingly larger eccentricities, and in Figure 1 is shown the distribution of the eccentricities of 111 planets³ discovered at present day. The figure exhibits that more than 50% of the planets have the eccentricities larger than 0.30, and HD 80606 b (Naef et al. 2001) can occupy the eccentricity amounting up to 0.93, which indicates that such unusual discoveries are quite different from the circumstances in our solar system, where most of the major planets revolve around Sun on the near-circular orbits. In addition, from the view of the observations, the larger eccentricities seem to favor the planet detectability, where the semi-amplitude of wobble velocity $K \propto M_p \sin i / \sqrt{a(1 - e^2)}$ (with $M_p \ll M_c$), herein M_c , M_p , a , e and i are, respectively, the stellar mass, the planetary mass, the orbital semi-major axis, the eccentricity and the inclination of the orbit relative to the sky plane, requires more massive planetary mass (\sim the order of Jupiter’s mass), a lower a (e.g., close-in giant planets) and a higher e (see Fig. 1). Moreover, many previous authors have put forward diverse theories and possible mechanisms to interpret the evolution and origin of the orbital eccentricity variation in the exosystems: the disk-planet or planet-planet interaction

³The data were taken from <http://exoplanets.org>, as of Aug. 5, 2003

(Goldreich & Tremaine 1980; Weidenschilling & Marzari 1996; Lin & Ida 1997; Ford, Rasio, & Sills 1999) render the orbital migration of gas giant planets embedded in the protoplanetary systems (Lin, Bodenheimer, & Richardson 1996; Ward 1997; Bryden et al. 2000; Nelson et al. 2000) and the eccentricities are usually believed to excite to the observed values through complicated processes (Snellgrove, Papaloizou, & Nelson 2001; Kley 2003) or hybrid mechanisms (Lee & Peale 2002; Chiang, Fischer, & Thommes 2002) related to both the planetary migration and the resonant capture. Therefore, as a second objective, we intend to preliminarily make a discussion of the possible origin of the eccentricities or resonant configurations (see §5) for two planets of HD 82943. As a final part, in §6, we summarize our principal results and give a brief discussion.

2. Numerical setup

In the present work, we aim to numerically investigate the orbital motions for the two companions for HD 82943 in a three-dimensional space. And at first, let us bear in mind that the two companions of this system are assumed to be in the same orbital plane for our simulations except where noted. Here we adopt the best-fit orbital parameters from the web site of the Geneva Team. As is known, the two-Kepler fit produce five parameters set- $(K_i, P_i, e_i, \omega_i, T_{pi})$, where for each planet $i = 1, 2$, are the amplitude K_i , the orbital period P_i , the eccentricity e_i , the argument of periapse ω_i and the time of periapse passage T_{pi} . The Geneva Team presented two sets of the orbital data and hereafter we respectively call them Fit 1 and Fit 2. Here for Fit 1 of 107 observations (as of July 31, 2002) with the residual of 7.4 m/s, the data are listed here: $m_1 \sin i = 0.88 M_{Jup}$, $m_2 \sin i = 1.63 M_{Jup}$, $a_1 = 0.73$ AU, $a_2 = 1.16$ AU, $e_1 = 0.54 \pm 0.05$, $e_2 = 0.41 \pm 0.08$, $\omega_1 = 138 \pm 13^\circ$ and $\omega_2 = 96 \pm 7^\circ$, where hereafter the subscripts 1 and 2 denote the inner and outer planets, respectively. And Fit 2 were derived by fitting 142 observations (as of October 13, 2003, see also Mayor et al. 2004) with the residual of 6.8 m/s, the orbital parameters are presented: $m_1 \sin i = 1.85 M_{Jup}$, $m_2 \sin i = 1.84 M_{Jup}$, $a_1 = 0.75$ AU, $a_2 = 1.18$ AU, $e_1 = 0.38 \pm 0.01$, $e_2 = 0.18 \pm 0.04$, $\omega_1 = 124 \pm 3^\circ$ and $\omega_2 = 237 \pm 13^\circ$. Apparently, the eccentricities, semi-major axes, periapse arguments, true anomalies and others can act as key factors to determine the shape of the radial velocity curves. However, due to the large interaction between two planets in a low mean motion resonance, Laughlin & Chambers (2001) pointed out that short-term perturbations among massive planets in multiple planet systems (such as GJ 876, HD 82943) can result in radial velocity variations of the central star that differ substantially from velocity variations derived assuming the planets are executing independent Keplerian motions. On the other hand, the best-fit orbital solutions can vary a little from time to time provided that more updated observations were supplied or other elaborate fitting procedure was considered (Mayor et

al. 2004), or the velocity trend is removed due to the unveiling of an additional planet or more planets (Fischer et al. 2001) for a specific system. Therefore, at this stage, it is meaningful to study the dynamical characteristics of the system based on the subsequent points: (i) slightly varying the orbital parameters about the best-fit parameters by adding the uncertainties with direct integrations, (ii) seeking for the possible stable geometry for HD 82943 in parameter space, (iii) the dynamical mechanisms of retaining the system and (iv) the likely eccentricity or configuration origin for two planets, which motivate us to dedicate to this contribution.

Next, we continue to describe the means of preparation for the initial orbital data before we start the numerical integrations: for each planet, we usually need to obtain six orbital elements - the semi-major axis a , the eccentricity e , the orbital inclination I , the nodal longitude Ω , the argument of periastron ω and the mean anomaly M . Here, two groups of the initial orbital elements were produced on the basis of the data by Fit 1 and Fit 2. In each group, we assume that the semi-major axes of the two planets are always unchanged, say, for Fit 2, being 0.75 and 1.18 AU respectively. As we have indicated above, the two resonant planets are supposed to be coplanar for the initial configuration and the inclinations are both taken as small constant values not far from zero, e.g., 0.5° . The eccentricities and arguments of periapse are generated in the orbital parameters space in the proximity of the best-fit orbital solutions given the nominal observation errors. For example, for Fit 2, we take the observed eccentricities e_1 or e_2 to be centered, respectively, at 0.38 and 0.18, and randomly displaced by not more than 3σ , respectively, then we obtain the resulting initial eccentricities for integration. Still, we carried out similar steps to achieve the starting values of periapse arguments. The remained two angles of nodal longitudes and mean anomalies⁴ are randomly distributed between 0° and 360° . As a consequence, we obtained 100 orbits for each planet, to perform the integration of the planetary system, and each pair of the orbits was integrated for the time span of 10^7 yr, unless otherwise stated. Obviously, these orbits just lie in the neighborhood of the fitting parameters and represent the orbital motions quite close to the reality. Here we make study of the possible motion near the best-fit orbital solutions and expect that such investigations can be helpful to reveal some important dynamical features for the studied system or present valuable clues on the searching for other exosystems related to a 2:1 resonance.

⁴Laughlin G. and Lee M.H. (2003, private communications) pointed out to us that the mean anomalies and periapse arguments should perfectly match the radial velocities. Here, we choose proper values for M , ω and Ω , such that the linear combination of initial arguments can be close to the resonant configuration, this is reasonable, because the real system is observably stable and approximate to 2:1 MMR. And in Table 1 and 2, we present the orbital solutions where the measurement errors of $\Delta\omega = 0$ and $\Delta e = 0$, indicating that the eccentricities and periapse arguments are just equal to those by the Geneva Team.

With the N-body codes (Ji et al. 2002), we carried out the numerical integrations for the HD 82943 system. In our simulations, we adopted the mass of the host star to be $1.05 M_{\odot}$ for Fit 1, and $1.15 M_{\odot}$ for Fit 2. Under the assumption of $\sin i = 1$, the minimum masses of two companions are employed throughout the paper unless we state elsewhere. In addition, we utilized the time step to be one percent of the orbital period of the inner planet (HD 82943 c) in the integrations. The numerical errors were effectively controlled during the integration, with the local truncation error 10^{-14} for the time span of 10^7 yr, in the meantime the accuracy was also checked by the energy errors. In comparison, we also employed symplectic integrators (Feng 1986; Wisdom & Holman 1991) to integrate the same orbit to assure the results for some cases.

In the research of the planetary systems, the maximum Lyapunov characteristic exponent (LCE) is usually adopted to identify the regular or chaotic orbits, since the chaotic orbits are sensitively dependent on the initial conditions, corresponding to a positive LCE in the secular evolution. In this paper, we refer to the stability for the system means that the orbiting planets can remain periodic or quasi-periodic motions with bounded trajectories after the investigated time was done. We define the unstable orbits that either of the planets is ejected far away or moves too close to their parent star, and in our simulations, the integration was automatically ended when meeting the following criteria: (1) either of the eccentricities approaches unity, (2) either of the semi-major axes exceeds the factor of 2 or reduces half of the starting values, (3) either of the planets collides with the star or these planets do each other when entering the scope of the mutual Hill sphere.

3. Stable planetary geometry in 2:1 mean motion resonance

To begin the study of the stable resonant geometry in HD 82943, let us firstly recall several known facts in our solar system. One may be aware that the pair of Jupiter and Saturn is in a near 5:2 commensurability. In general, the mean motion resonance takes place in the pairs of the moons of the major planets (such as the Galilean satellites of Jupiter: Io-Europa-Ganymede; see Lee & Peale 2002), the asteroidal belt and Kuiper Belt Objects (KBOs) (Duncan, Levison, & Budd 1995; Wan & Huang 2001). As more and more extrasolar planetary systems are being discovered, the resonant pairs are frequently found to occur in the multiple systems, e.g., HD 82943 (Goździewski & Maciejewski 2001), GJ 876 (Lee & Peale 2002), and possibly HD 160691 (Goździewski, Konacki, & Maciejewski 2003; Bois et al. 2003) in a 2:1 MMR, and 55 Cnc in a 3:1 MMR (Ji et al. 2003a), and so on. Several theoretical or numerical works have been done to enhance the comprehension of the evolution into the resonances by non-conservative tidal forces (Ferraz-Mello, Beauge, & Michtchenko

2003), the convergent migration for the planets due to the disk-planet interaction by a damping force (Snellgrove et al. 2001; Lee & Peale 2002; Kley 2003), the excitation of the orbital eccentricities by repeated crossings of two companions migrating on divergent orbits (Chiang et al. 2002; Chiang 2003) or the eccentricity growth by two resonant planets through inward migration (Murray, Paskowitz, & Holman 2002), and resonant inclination excitation mechanism for migrating planets in the gas disk (Thommes & Lissauer 2003). On the other hand, if the two planets are trapped into a 2:1 resonance via one of the potential mechanisms, it is still necessary to understand their actual situation of orbital motions after the capture, and to investigate whether they can secularly survive in the system in some appropriate geometry and examine how the stability depends on the orbital parameters.

In the usual notation of celestial mechanics, the lowest order eccentricity-type (see Murray & Dermott 1999) resonant arguments θ_1 , θ_2 for the 2:1 MMR are

$$\theta_1 = \lambda_1 - 2\lambda_2 + \varpi_1, \quad (1)$$

$$\theta_2 = \lambda_1 - 2\lambda_2 + \varpi_2, \quad (2)$$

where λ_1 , λ_2 are , respectively, the mean longitudes of the inner and outer planets, and ϖ_1 , ϖ_2 denote their apsidal longitudes, respectively. Additionally, the relative apsidal longitudes of two companions θ_3 reads,

$$\theta_3 = \varpi_1 - \varpi_2 = \Delta\varpi. \quad (3)$$

As we mentioned previously, the apsidal alignment (or antialignment) is found to exist in most of the multiple systems (Kinoshita & Nakai 2000; Rivera & Lissauer 2000; Chiang, Tabachnik, & Tremaine 2001; Laughlin et al. 2002; Lee & Peale 2002, 2003; Gozdziewski et al. 2003; Ji et al. 2003a, b; Zhou & Sun 2003), to play a significant role in retaining the stability of the system (Gozdziewski 2003; Ji et al. 2003b). Moreover, this apsidal phase-locking of two orbits indicates that a pair of planets have common time-averaged rate of apsidal precession, and in the literature, it is also referred to apsidal resonance or corotation (Chiang et al. 2001; Malhotra 2002). For a 2:1 MMR, it is easily noticed that for the above three arguments, no more than two are linearly independent, indicating that either all three librate or only one librate in the occurrence of the libration of the critical argument. In more general case, Nelson & Papaloizou (2002) also showed that both situations can occur for a $p : q$ eccentricity-type commensurability (Murray & Dermott 1999), where the associated resonant angles are defined by $\phi_{p,q,k}(\lambda_1, \lambda_2, \varpi_1, \varpi_2) = p\lambda_1 - q\lambda_2 + (k-p)\varpi_1 + (q-k)\varpi_2$ (p, q, k are positive integers and $p \leq k \leq q$) in the numerical surveys of the pair of the extrasolar planets. As a matter of fact, this was again verified in the case of the 3:1 MMR for 55 Cnc (Ji et al. 2003a; Zhou et al. 2004), where not only do all three resonant angles of $\lambda_b - 3\lambda_c + 2\varpi_c$, $\lambda_b - 3\lambda_c + \varpi_b + \varpi_c$ and $\lambda_b - 3\lambda_c + 2\varpi_b$ (here the subscript b, c, respectively, denote the two

inner planets of 55 Cnc b and 55 Cnc c) librate, but the relative apsidal longitude of $\Delta\varpi$ librates about a constant angle simultaneously.

In the simulations of HD 82943, we found that three types of stable orbits can survive in this system: (I) Only θ_1 librates about 0° , while θ_2 and θ_3 circulate; (II) Case of alignment, three arguments all librate about 0° , denoting by $\theta_1 \approx \theta_2 \approx \theta_3 \approx 0^\circ$; (III) Case of antialignment, both θ_1 and θ_3 librate about 180° , while θ_2 librates about 0° , denoting by $\theta_1 \approx 180^\circ$, $\theta_2 \approx 0^\circ$, $\theta_3 \approx 180^\circ$. In the following sections, we will separately discuss above three stable configurations with both the numerical outcomes and analytical means and also compare them with remarkable evidences in other multiple systems involved in 2:1 resonance.

3.1. Coplanar semi-analytical model

First, let us suppose two planets with the masses of m_1 and m_2 orbit the central star with the mass of m_0 . Here we only take into account the point-mass interaction between star-planet and planet-planet, without the consideration of the effects of the oblateness and general relativity arising from the parent star. Thus, in Jacobi coordinates ($a_i, i = 1, 2$; assume $a_1 < a_2$), the Hamiltonian for three-body system can be written (Brouwer & Clemence 1961):

$$F = F_0 + \Phi, \quad (4)$$

where

$$F_0 = -\frac{Gm_0m_1}{2a_1} - \frac{Gm_0m_2}{2a_2}, \quad (5)$$

and

$$\Phi = -\frac{Gm_1m_2}{r_{12}} - Gm_0m_2 \left(\frac{1}{r_{02}} - \frac{1}{r_2} \right). \quad (6)$$

Here r_{02} (or r_{12}) is the distance between m_0 (or m_1) and m_2 , r_2 the distance of m_2 with respect to the center of mass for m_0 and m_1 . Therefore, the disturbing potential Φ can be further expanded to the following forms for the coplanar case,

$$\Phi = -\frac{Gm_1m_2}{a_2} \sum S(a_1, a_2, e_1, e_2) \cos \phi, \quad (7)$$

where

$$\phi = k_1\lambda_1 + k_2\lambda_2 + k_3\varpi_1 + k_4\varpi_2, \quad (8)$$

Here

$$\sum_{i=1}^4 k_i = 0. \quad (9)$$

In (7), S depends on the semi-major axes (in association with the Laplace coefficients) and the eccentricities of two planets and this expansion of the disturbing potential also requires the smaller values of e_i ($i=1,2$) and the two orbits without intersection. In the case of GJ 876, Lee & Peale (2002) expanded (7) and collected the terms up to e^3 , the truncation series may be valid for low values of e_i , where $e_1 = 0.255$ and $e_2 = 0.035$ (Laughlin & Chambers 2001), without the occurrence of the crossing orbits. In a more recent work, Beauge & Michtchenko (2003) also developed an expansion method that can deal with higher values of the eccentricities up to a limit of $e_i \sim 0.5$, but they suggested that it is still related to the situation of the proximity between the planets. However, as for HD 82943, the planetary eccentricities can be as high as 0.41-0.54 for Fit 1, or 0.18-0.38 for Fit 2, the development of (7) with respect to large eccentricities cannot be exactly applied, because the expanding series, consisting of a great number of the expansion items, either converge very slowly or become divergent in the collision circumstances. Therefore, herein we seek for a semi-analytical treatment (Kinoshita & Nakai 2002) for this question and then compare the analytical results with direct numerical integrations. We emphasize that this semi-numerical method corresponds to a first-order theory with respect to the small parameter ϵ , where ϵ represents the mass ratio of the Jupiter-like planet to its parent star and is normally of the order of $\sim 10^{-3}$ in the planetary systems, and can apply to the planetary system with any eccentricities, even for the mutual crossing case.

The Hamiltonian for the coplanar case is

$$F = F(a_1, a_2, e_1, e_2, \varpi_1, \varpi_2, \lambda_1, \lambda_2). \quad (10)$$

In order to keep the Hamiltonian form, we should use Jacobi coordinates to study this system. As the indirect part of the Hamiltonian F does not contribute to the secular part, we simply take the direct part. As the two orbits of HD 82943 are close to each other and may intersect (Ji et al. 2003c; Hadjidemetriou & Psychoyos 2003; Lee 2004), the ordinary analytical expansions of the main part invalidate in the practical usage, then we adopt the original form of the main part of the disturbing function and numerically evaluate it. Again, by eliminating short-periodic terms in the classical average process, the new Hamiltonian reads:

$$F^* = F^*(a_1, a_2, e_1, e_2, \theta_1, \theta_3). \quad (11)$$

The degree of freedom of the new Hamiltonian (11) is reduced from four to two. However, the Hamiltonian F^* is not integrable. As we shall see in §3.2 that the semi-major axes of the two resonant planets slightly change when they are close to 2:1 MMR, so we can assume that a_1 and a_2 are almost constant (see Figures 2 and 3) for the critical argument $\theta_1 = 0^\circ$ or $\theta_1 = 180^\circ$. In final, the degree of freedom of the new Hamiltonian is reduced to one:

$$F^* = F^*(e_1, e_2, \theta_3). \quad (12)$$

We again eliminate e_2 in equation (12) with conservation of the total angular momentum J (see also Appendix), then we have

$$F^* = F^*(e_1, \theta_3, J). \quad (13)$$

Thus we can draw the level curves of the Hamiltonian and understand the global behavior of e_1 and θ_3 . As the eccentricity e_1 of the inner planet becomes large, we numerically averaged the original Hamiltonian (10) under the condition of the critical argument $\theta_1 = 0^\circ$ or $\theta_1 = 180^\circ$ and the angular momentum conservation relationship, and then obtain numerically the averaged Hamiltonian (13) with the parameter of the total angular momentum J . The technique of the numerical averaging is extensively described in the paper (Kinoshita & Nakai 1985), in which the case of $\theta_1 \neq 0$ is also discussed. To make a study of the evolution of the eccentricities and the relative periaapse arguments, we can draw the contour map of Hamiltonian (13) by taking θ_3 as the horizontal axis and e_1 or e_2 as the vertical axis (see Figure 4) with the parameter J , which is determined from the initial conditions.

3.2. Results for Fit 1

For the first 100 runs for Fit 1, each orbit integration lasts for $t = 10^7$ yr. In the simulations, we notice that all the stable cases are involved in the 2:1 MMR and easily understand that the stability of a system is sensitive to its initial planetary configuration. Furthermore, we noticed that 2%, 3%, and 2% of the cases belong to Types I, II, and III and 93% of the systems destabilize, which means that either of the two planets leave *in situ* to the infinity with a rapid increase of the semi-major axes or the eccentricities grow much larger on the timescale $\sim 10^4 - 10^5$ yr or even shorter, owing to the mutual interaction between star-planet or planet-planet through frequent close approaches. In Table 1, are listed two sets of orbital parameters—Fit 1a is related to the antialigned configuration for Type III and Fit 1b is involved in the case for aligned orbits for Type II. Here the adopted parameters for two planets are the masses of 1.63-0.88 M_{jup} , the semi-major axes of 1.16-0.73 AU, the eccentricities of 0.41-0.54. Let us first examine the stable orbits of Type I, where in the numerical simulations, we find that only one argument of θ_1 librates about 0° and the others θ_2 and θ_3 take up the full circulation from 0° to 360° . The semi-major axes a_1 and a_2 perform tiny oscillations about 0.73 and 1.15 AU for the whole integration time. Type I was initially introduced by Goździewski & Maciejewski (2001) with the previous fits. However, in this paper, Types II and III, which can grasp the couple of companions escaping from deviating their tracks in two directions of remaining both the semi-major axes and the eccentricities, are new findings of stable orbits for this resonant system. Hence, in the following sections, we primarily pay attention to the stable configurations linked to both a 2:1 resonance and

the apsidal corotation.

3.2.1. Antialigned case

Figure 2 shows the typical orbital evolution for Fit 1a (antialigned orbits). In the figure, we can see that the semi-major axes a_1 and a_2 slightly vibrate about 0.73 and 1.15 AU for $t = 10^7$ yr⁵ (in the figure, to see more clearly, we simply display a snapshot for $t = 2000$ yr), meanwhile θ_1 librates about 180° with a moderate amplitude of $\sim 30^\circ$, θ_2 about 0° with a smaller amplitude of $\sim 10^\circ$ and θ_3 (by *thick line*) about 180° with an amplitude of $\sim 30^\circ$. It is noteworthy to point out that the 2:1 resonance variable θ_1 librates in accord with the relative apsidal longitudes θ_3 , occupying the same period of ~ 300 yr. This phenomenon can be easily understood because the above three angles are not independent in the course of the orbital motion. Thus we can call θ_1 and θ_3 as two fundamental variables to characterize the stable planetary geometry in 2:1 MMR. In addition, the modulations of the semi-major axes a_i and θ_i ($i = 1, 2$) reveal the fact that the two planets are indeed trapped in a 2:1 MMR for the secular orbital evolution. In Figure 2, we further notice that the eccentricities of e_1 and e_2 separately range in (0.36, 0.56) and (0.39, 0.49), bearing the equal libration periods of θ_1 and θ_3 . The orbital antialignment of axes in HD 82943 is reminiscent of that in the 2:1 orbital resonances for Io-Europa system (Lee & Peale 2002), in which θ_1 (involved in the Io’s longitude of periapse) librates about 0° , and θ_2 (involved in the Europa’s longitude of periapse), θ_3 librate about 180° , respectively. The antialigned circumstance for Io-Europa is equivalent to Type III in the sense of dynamically stable configuration, however, these jovian moons are occupying almost near-circular orbits resulting from the primordial or the tidal origin (Peale 2003) and the resonance configuration may come into reality when the eccentricities are small. By contrast, the HD 82943 system differs the Io-Europa pair in that both of the planets possess high eccentricities at present day. Hence, the origin of the 2:1 resonance for HD 82943 (Fit 1a) orbiting two massive planets with elliptic trajectories should be explained by an innovative mechanism rather than a capture induced by co-orbital differential migration (S. Peale 2003, private communication; see also §5) and perhaps stem from gravitational scattering in a crowded system that augment their eccentricities, i.e., for a system with 10 planets (Adams & Laughlin 2003), the scattering processes can yield the full extent of possible eccentricity where $0 \lesssim e \lesssim 1$.

Recently, Bois et al. (2003) found that the stable configuration of the HD 160691

⁵We also extend the integration to 10^8 yr using symplectic integrator for this case, and no sign shows that the system will become chaotic for longer evolution.

system is possibly involved in a 2:1 mean motion resonance combined with an anti-aligned in two apsidal lines, with higher eccentricity ($e_2 > 0.52$) of the outer planet. Obviously, their research supported the stable geometry of Type III of HD 82943, which also implies that this resonant topology may be suitable especially for the planets bearing larger eccentricities.

Moreover, this antialigned resonant configuration for Fit 1a means that the conjunctions can take place when the inner planet moves near apoapse and the outer planet is close to the periapse, and *vice versa*, which indicates that the two planets are far from each other during their orbital evolution and protected from frequent close encounters. Therefore, we can safely conclude that the stability of the HD 82943 system, which is related to the above coplanar configuration for Fit 1a, can be simultaneously sustained by two dynamical mechanisms: the 2:1 MMR and the apsidal antialignment.

3.2.2. Aligned case

Figure 3 exhibits the orbital evolution for Fit 1b (aligned orbits). Consequently, let us note that the semi-major axes a_1 and a_2 do not change dramatically but undergo small oscillations about 0.73 AU and 1.15 AU for $t = 10^7$ yr (a snapshot for $t = 3000$ yr), further the eccentricities e_1 and e_2 librate in the extent of (0.5, 0.8) and (0, 0.45), respectively, in the behavior of the converse cycles, owing to the conservation of the total angular momenta for the system. Here θ_1 librates about 0° with a small amplitude of $\sim 20^\circ$, but θ_2 and θ_3 (by *thick line*) individually librate about 0° with a large amplitude of $\sim 70^\circ$. In this resonant aligned geometry, we again observe that θ_1 , θ_2 and θ_3 share the common librating period of ~ 700 yr, in the same time, coupled with the librating period of the eccentricities of e_1 and e_2 . In addition, it is worthwhile to point out that at the time that θ_1 , θ_2 and θ_3 all approach zero (where θ_1 and θ_3 start from the negative values to zero), the eccentricity of e_1 reaches the maximum ~ 0.8 and e_2 is close to the minimum ~ 0 , thus at the aligned conjunction point, the separation between two planets $d = a_2(1 - e_2) - a_1(1 - e_1)$ (where a_1 and a_2 are almost preserved on the condition of 2:1 resonance locking) can reach the maximal value and the maximum separation can prevent them from strong mutual perturbation when they rendezvous at the synodic location. Similar analysis can be applied for the case of Fit 1a, where both θ_1 and θ_3 run through 180° (see Figure 2). Again, let us make a brief comparison with the circumstance for the 2:1 resonant system GJ 876, which is also found to be in aligned configuration for the two orbits (Marcy et al. 2001). Lee & Peale (2002) further found that the amplitude of the librations of three arguments are not far from 0° by using Laughlin-Chambers solutions and they even indicated that all the librations are remained even for the amplitudes of θ_1 amounting up to 45° for some cases. As for Fit 1b, let us bear in mind

the fact that the planetary eccentricities are much larger than those for GJ 876, although they may have similar planetary orbital geometry. Sequently, the conjunctions always take place when two planets move close to their the periapse longitudes and the alignment can be maintained over long-term orbital evolution. This, *de facto*, reveals that Type II coplanar configuration may be possible for real observed systems of GJ 876 and HD 82943.

3.2.3. Comparison with the semi-analytical results

Here we adopted the semi-analytical model introduced in §3.1 to draw the Hamiltonian contour and then compare these results with those given by direct integrations over secular orbital evolution. In the averaged Hamiltonian after removing the short-periodic terms, the difference arising from the choice between the Jacobi coordinates and astrometric coordinates is the order of the perturbation $(m_1/m_0, m_2/m_0)$, which could be ignorable. Therefore, we adopt the astrometric elements given in Table 1 to be Jacobi elements in the averaged model. As a comparison, the initial orbital elements for numerical integration are also converted into the Jacobi coordinates. In Figure 4, we indicate that the contour diagram of Hamiltonian (13) are plotted against various levels by changing e_1 , e_2 and $\Delta\varpi = \varpi_1 - \varpi_2$, *left panel* represents the results for Fit 1a, where the contour levels are exhibited by *thin line* and the numerical solutions shown by *thick line* (the innermost curve about marked *plus*), while *right panel* for Fit 1b. The $e_i - \Delta\varpi$ figures show a good agreement between the numerical outcomes and the semi-analytical solutions for two fits. It is worthwhile to mention that the closest level of the Hamiltonian contour to the numerical solution set the stable boundary for the apsidal resonant geometry, inside which the regular orbital motion for two orbits can be found with qualified eccentricities and the relative apsidal longitudes, thus we may conclude that this semi-analytical means is effective to help predict stable orbital solutions (e.g., Beauge et al. 2003). On the other hand, the diagrams of the Hamiltonian contour further show that the stability zones for the eccentricities e_1 and e_2 are connected with the librating amplitude of $\Delta\varpi$: the smaller stability zones of the eccentricities, the narrower modulations of the relative apsidal longitudes, and *vice versa*.

In addition, we calculated the equilibrium points for each fit: $(180^\circ, 0.45)$ and $(180^\circ, 0.46)$, respectively, for Fit 1a; $(0^\circ, 0.68)$ and $(0^\circ, 0.29)$, respectively, for Fit 1b. As for Fit 1b, we observe that there should exist stable orbits about the equilibrium center for $(\Delta\varpi, e_2) = (0^\circ, 0.29)$, together with high eccentricity e_1 above 0.60, which satisfy the necessary conditions for two planets evolving into a 2:1 resonance (Kley, Peitz, & Bryden 2004; see also §5). Again, we recall that the period of the 2:1 resonant variable θ_1 is equal to that of the relative apsidal longitudes θ_3 (see Figs. 2 and 3), which can be clearly reflected in

Fig. 4. Moreover, in a view of the numerical results, we can see that the eccentricities of both planets are well restricted with the small-amplitude libration of θ_3 about 180° for Fit 1a (antialigned) and large-amplitude libration of θ_3 about 0° for Fit 1b (aligned), which can also be consistent with the results in Figs. 2 and 3.

As aforementioned, different selections for the initial orbital parameters will lead to stable or unstable configurations for the HD 82943 system. By analyzing the starting orbital data, we discover that those stable planetary orbits involved in Type II (or III) require the initial θ_1 and θ_3 should be constructed to satisfy the conditions of being less than tens of degrees from 0° (or 180°), implying that the linear combinations of the mean anomalies, ascending nodes and periapse arguments can be close to the 2:1 resonant geometry.

3.3. Results for Fit 2

As for the second 100 runs near the vicinity of Fit 2, we found there exist two kinds of stable geometry related to a 2:1 MMR for this new fit (Mayor et al. 2004), in which 16% of the stable systems can last for 10^7 yr (where 14% of the stable cases is in aligned orbits of Type II and 2% with simply θ_1 libration for Type I), and 84% are found to self-destruct at $t < 10^6$ yr. The percentage of the survival orbits indicates that there is a likelihood for the two planets of this system to be aligned. In Table 2, are listed the orbital parameters in association with the alignment of two orbits. Let us recall the adopted planetary masses of 1.84-1.85 M_{jup} , the semi-major axes of 1.18-0.75 AU and the eccentricities of 0.18-0.38. In the following subsections, the additional computations are carried out most frequently according to the initial orbits from Fit 2, and the typical secular evolution timescale ranges from 10^6 yr to 10^7 yr.

Figure 5 illustrates the typical aligned orbital evolution for Fit 2. In comparison with Figure 3, we notice that the semi-major axes a_1 and a_2 are almost unchanged but modulate about 0.75 and 1.18 AU with small amplitude for $t = 10^7$ yr, at this time, the amplitude of the oscillations for e_1 and e_2 are not so large and the eccentricities are just wandering in the span (0.34, 0.44) and (0, 0.25), respectively. Here θ_1 librates about 0° with a moderate amplitude of $\sim 45^\circ$ (in coincidence with one of the aligned case for GJ 876 found by Lee & Peale 2002; see also §3.2.2), but θ_2 and θ_3 (by *thick line*) individually librate about 0° with large amplitude of $\sim 80^\circ$. Again, we notice that the eccentricities have the libration periods of ~ 600 yr, which are coupled with those of θ_1 and θ_3 . It should mention that although the various starting orbital parameters between Fit 2 and Fit 1b can result in variational librating amplitudes in the eccentricities and resonant arguments, however, from a viewpoint of topology, there is not so much difference between two aligned orbital solutions.

Furthermore, in Figure 6, we still plot $e_i - \Delta\varpi$ Hamiltonian contour (by *thin lines*) and the numerical results are presented by dotted points. The equilibrium solutions (by *plus*) are: $(0^\circ, 0.40)$ and $(0^\circ, 0.13)$, respectively. The semi-analytical contour chart exhibits a good agreement with the numerical investigations of maintaining the eccentricities with larger θ_3 -libration amplitudes. On the other hand, the figure implies that the θ_3 -libration will be broken up if the libration amplitudes exceed or approach the critical value of 90° near the separatrix, then two successive scenarios may occur, either aligned orbits evolve into Type I geometry that simply θ_1 librates, or the system destabilize on the shorter timescale. In the sense of the present solutions, the aligned configuration for HD 82943 is not robust than the antialigned case, where a wider relative periaapse longitudes can be initially adopted (see Figure 4). Bois (2003, private communication) also confirmed that the stable strip of the alignment for the initial $\varpi_1 - \varpi_2$ is much narrower than that of the antialignment in their numerical calculations for HD 82943. However, if the aligned orbits are close to librating center, the robustness can be strengthened with a different story.

In order to distinguish the dynamical behaviors in orbital parameter spaces and explore how the stability zones dependence on these parameters, we extensively perform abundant integrations for each series (where in each series, we only allow one parameter vary but others keep unchanged) to numerically search for the stable solutions. In the following sections, we will discuss these results respectively.

3.3.1. Dependence on the semi-major axes

Figure 7a show the numerical scanning of the HD 82943 system in the semi-major axes space of $[a_1, a_1]$. All other orbital parameters are taken from Table 2. In this group of the simulations, we choose $a_1 \in [0.60 \text{ AU}, 0.80 \text{ AU}]$ and $a_2 \in [1.00 \text{ AU}, 1.30 \text{ AU}]$ with the resolution of 20×20 grids, each direction spaced 0.01 AU. In Fig. 7a, the cross indicates the unstable orbits and the filled circles for stable orbits that the planets survive at least 10^6 yr. Here, we notice that there exists a stable strip with the width from ~ 0.01 AU to ~ 0.02 AU, indicating that these stable solutions are quite close to the 2:1 resonance. Meantime, the intersection between the vertical and horizontal lines represents for the present solution from Fit 2, which is well located in the stable map.

In the case of 2:1 resonance, we have $a_2/a_1 = (P_2/P_1)^{2/3}$, where $P_2/P_1 \simeq 2$, if both of orbits contract or expand k times of the initial configuration (e.g., Fit 2) and the planetary masses becomes \sqrt{k} of the initial masses (where other orbital parameters remained), the semi-amplitude of the radial velocity will not change, that's the reason why we can see a linear stable ribbon in Fig. 7a. In this sense, the semi-major axes cannot be uniquely

determined unless their orbital periods are previously obtained from the observations.

3.3.2. Dependence on the eccentricities

Mayor et al. (2004) pointed out that one should be careful of employing the newly updated orbital fits (Fit 2) due to the derived best-fit solutions of lack of considering the planet-planet interaction. Hence, the exploration for the orbital parameter space is extremely useful to help understand the stability regions relying on the eccentricities. Similar to the numerical scanning in the semi-major axes space, here only both of the eccentricities of e_1 and e_2 are allowed to be free parameters. In this series of the investigations, we let $e_1 \in (0.0, 0.60)$ and $e_2 \in (0.0, 0.60)$ and the resolution in $[e_1, e_2]$ space is 20×20 points, spaced 0.03 in each grid (see Figure 7b), the integration time is 10^6 yr for each orbit. In the figure, the symbols are defined as in Figure 7a, where the filled circles mean those orbits are steady over secular evolution.

According to the eccentricity of the outer planet e_2 , we summarize the results as follows:

- (1) strongly stable cases, where $0 < e_2 \leq 0.24$ (40%),
- (2) partially stable cases, where $0.24 < e_2 \leq 0.39$ (16% stable, 9% unstable),
- (3) unstable cases, where $0.39 < e_2 < 0.60$ (35%).

As for case (1), we should mention two points: firstly, the eccentricities of Fit 2 (shown by the crossing of two lines) just reside in the stable map of $[e_1, e_2]$; secondly, in this figure, we notice that there exist stable solutions when $e_1 = 0.4$ and $e_2 \simeq 0$, which is consistent with Mayor et al. (2004), who also provided the other solution involved in an aligned configuration with a near-circular orbit for outer planet but found the residuals do not dramatically change. We can also note that a higher e_1 can be possible in this system. Both of cases (1) and (2) contain more than 50% of the stable orbits in the numerical scanning, exhibiting that only a moderate e_2 will favor the stability of the HD 82943.

The case (3) shows that when e_2 becomes larger than 0.39, no regular orbits will appear even though e_1 can be adopted to be small values, which suggests that in this situation the stability for HD 82943 is more sensitive to the orbital motion of the outer planet, which can greatly determine whether the system is in chaotic or regular status.

3.3.3. Dependence on the mean anomalies and arguments of periapse

Figures 7c and 7d exhibit our numerical exploration in the parameter spaces of $[M_1, M_2]$ and $[\omega_1, \omega_2]$ for the time span of 10^6 yr, respectively, with the resolution of 18×18 grids. The stable map in the $[M_1, M_2]$ space again show the condition of the 2:1 MMR, where there is a linear relationship $M_1 = 2M_2 + \text{const}$. Therefore, on the basis of Fig. 7c, we can not only verify our original mean anomalies of Fit 2 (by intersection) but find the other arguments related to stable orbital motions for two planets. The stable diagram in the $[\omega_1, \omega_2]$ space reveals the fact that both of the apsidal longitudes of ϖ_1 and ϖ_2 (where nodal longitudes are constant here) precess at the equal rate about the star. The stable zones in Fig. 7d are quite narrower, as we stated before, this results from the aligned configuration with a larger libration of $\theta_3 \sim 80^\circ$ (ref. Fig. 5). Both figures clearly illustrate that those stable configurations are linked to the 2:1 resonance and apsidal corotation.

3.3.4. Dependence on the planetary mass ratio

In this section, we expect to understand how the stability depends on the planetary mass ratio for the coplanar planetary configurations. Here in our numerical study, we still adopted the orbital elements from Table 2, except the masses of two planets m_1 and m_2 . Firstly, we varied $\sin i$ in an incremental step of 0.05 ranging from 0.35 to 1.00, and the rescaled masses of m_k ($k = 1, 2$) can conveniently be obtained by the product of $m_k \sin i$ for a specific $\sin i$, where the mass ratio m_1/m_2 is fixed to be $1.85/1.84 \sim 1$. Then 14 coplanar integrations were carried out for 10^7 yr in this runs. The numerical results show that the stable orbits (of Type II) for HD 82943 requires $\sin i \geq 0.50$. The stability set limitations on the planetary masses where $m_1 \in [1.85M_{Jup}, 3.70M_{Jup}]$ and $m_2 \in [1.84M_{Jup}, 3.68M_{Jup}]$ for different values of $\sin i$. In the case of GJ 876, similarly, Marcy et al. (2001) reported that several stable systems, catalogued in Type II, had $\sin i = 0.50$ for the integration timescale up to 500 Myr. Additionally, Laughlin & Chambers (2001) also suggested that $\sin i$ possibly ranges from 0.5 to 0.8 for the coplanar fits for GJ 876. From above statements, we notice that $\sin i \geq 0.50$ is necessary for both systems occupying a 2:1 resonance and the extent of the planetary masses can further be estimated.

In the other computations, we changed the mass ratio for m_1/m_2 and fixed the mass $m_2 = 1.84 M_{jup}$, let $m_1/m_2 \in [1/4, 4]$, then performed over thirty additional simulations to explore the stability of the system depending on the variational mass ratios. As a result, we found that $m_1/m_2 \leq 2$ is necessitated for the stable orbits, indicating an upper limitation for the mass of the inner planet when we remain that of the outer companion. In the following step, we replaced m_1 with much lower masses ranging from several M_\oplus to $20 M_\oplus$ for new

investigations, and found that the stable geometry of Type II can still be remained and a surprise is that the eccentricity of the inner planet can amount up to ~ 0.90 with quasi-periodic oscillations. These numerical explorations suggest that the apsidal configuration can maintain with much smaller masses for inner planet, which is consistent with the results given by Beauge et al. (2003), who analyzed the corotational solutions by gradually decreasing the mass of the inner planet and found that although the solutions simply depend weakly on the individual masses of the planets and the maximum value for the planetary mass of m_1 is indeed in existence with given eccentricities for the stable apsidal topology.

3.3.5. *Dependence on the relative inclination*

In our solar system, most of the major planets have small inclinations with regard to the essential reference plane. However, there is a special case for the Neptune-Pluto system ($M_{Neptune} \approx \frac{1}{5}M_{Saturn}$), where Pluto orbit an eccentric trajectory with a large inclination of $\sim 17^\circ$ but Neptune travels on a near-circular orbit with the inclination less than 2° (Murray & Dermott 1999). Cohen & Hubbard (1965) discovered that these two planets are involved in a 3:2 resonance with the argument $3\lambda_P - 2\lambda_N - \varpi_P$ ($\lambda_{P,N}$ denote, respectively, the mean longitudes of Pluto and Neptune, ϖ_P is the longitude of perihelion of Pluto). These studies reveal that there may exist a relative inclination configuration between two orbits in association with the mean motion resonance. In this sense, we anticipate to understand the situation for the present exosystem.

We again performed extra tests of mutually inclined orbits for two resonant planets for the integration of 10^7 yr, to examine the stability of the HD 82943 system. The orbital data were taken from Table 2 and for simplicity, we just adopt their minimum masses and remain them unchanged for our additional integrations. For the initials, here we simply altered the inclination of the outer planet I_2 and increased I_2 in an increment of 5° from 5.5° to 85.5° , but always assumed the inclination of the inner planet I_1 to be 0.5° . The numerical integrations reveal the fact that although the inclination was greatly changed, the two planets are still in 2:1 MMR and apsidal alignment (Type II) with the inclination of $I_2 \leq 25.5^\circ$. On the contrary, for $I_2 > 25.5^\circ$, we found that the eccentricity of the inner planet can pump up to unity due to the great perturbation exerted by the outer planet and leave the orbits eventually. The relative inclination i_r can be determined by $\cos i_r = \cos I_1 \cos I_2 + \sin I_1 \sin I_2 \cos(\Omega_1 - \Omega_2)$, where Ω_1 and Ω_2 are, respectively, the longitudes of ascending nodes for two planets. To sum up, in the case of the non-coplanar configuration for HD 82943, stability requires that the relative inclination be $\sim 25^\circ$ or less. In the case of GJ 876, Rivera & Lissauer (2001) carried out dynamical fits for the possible best solutions for the mutual inclination geometry

and found that the stability for GJ 876 requires the relative inclination to be 12° or less. Therefore, it should be mentioned that the mutually inclined orbits dynamically survive over long-term timescale in the planetary geometry locking into a 2:1 MMR, but it should place constraints on the initial conditions for two planets. Thommes & Lissauer (2003) showed that two planets migrating in resonance can perform significant excitation of their inclinations and the relative inclination between two planets can grow to $\sim 30^\circ$ in their three-dimensional simulations. As a final note for this part, the above-mentioned numerical investigations for various mutual inclined exosystems show that the low relative inclination do play an important role in the stability for such systems, and this mutual inclined configuration may arise from the inclination-type resonance (Thommes & Lissauer 2003) associated with the longitudes of the ascending nodes for inner and outer planets if the inner planet owns a high eccentricity (e.g., for Fit 2, $e_1 = 0.38$), while the higher relative inclination geometry can destabilize the system (e.g., Lissauer & Rivera 2001) on shorter timescales.

3.4. Comparison with other works

As we mentioned previously, several studies have been devoted to explore the orbital motions of the exosystems in 2:1 MMR. In the case GJ 876, Lee & Peale (2002) discovered that there are stable configurations with θ_1 , θ_2 and θ_3 all librating about 0° (related to Type II) for $0.15 \lesssim e_1 \lesssim 0.86$, and Kinoshita & Nakai (2001) and Ji et al. (2002) also studied this system and confirmed the 2:1 resonance acting as an effective mechanism to hold the system, moreover, an extended stable geometry of Type I was shown by Ji et al. (2003b) for GJ 876. In other works, Hadjidemetriou & Psychoyos (2003) numerically studied the families of periodic orbits for HD 82943 in the rotating frame, and indicated that two kinds of families orbits can survive for the 2:1 resonant planets in their computations. However, it is the first time that we show an exhaustive exploration in the orbital parameter space for the HD 82943 system based on the updated solutions, which reveals the new dynamical features for this system.

In summary, the results presented in this article on the possible stable planetary geometry involved in a 2:1 resonance are not only consistent with the previous studies, but also outline an extensive dynamics of these systems. Moreover, we point out that the aforementioned three groups of resonant configurations imply a general principle that governs two planets in a dynamically stable state over secular orbital evolution in the planetary systems, which should be examined by more future discoveries of the 2:1 resonant pairs. Still, we will concentrate on whether a postulated terrestrial can survive in such geometry (see §4), and how a certain system is evolved into an apsidal alignment or antialignment resonant

configuration in §5.

4. Habitable zones

The Habitable zones (HZ) are generally convinced to be suitable places for terrestrial planets that can provide the liquid-water, subtle temperature and atmosphere environment, and other proper conditions (Kasting et al. 1993), supporting the development and biological evolution of life on their surfaces. The habitable region is considered to be centered at $a_p = 1 \text{ AU } (L/L_\odot)^{1/2}$ (Gould, Ford, & Fischer 2003) or $a_p \geq 1.03 \text{ AU } (L/L_\odot)^{1/2}$ (Kuchner 2003), such that a water planet can exist in equilibrium with stellar radiation, where a_p is the radius of the planet’s orbit and L is the luminosity of the host star. In a viewpoint of the dynamics, first of all, there should be stable orbits at $\sim 1 \text{ AU}$ for Earth-like planets moving about main sequence stars over very long timescale and we can also refer this to the dynamical habitability. In a recent work, Menou & Tabachnik (2003) exhaustively studied the dynamical habitability of 85 known extrasolar planetary systems through numerical simulations of their orbital dynamics in the presence of potentially habitable terrestrial planets. They found that more than half of the known exosystems cannot harbor habitable terrestrial planets and about 25% of the systems mostly with close-in giant planets are dynamically habitable, similar to our solar system. And in this section, we only draw our attention to the potential habitable zones for the systems (e.g. HD 82943 and GJ 876) with a stable geometry in a 2:1 resonance.

Here we performed numerical surveys in examining the Habitable zones both for HD 82943 and GJ 876. And at first, we considered stable configurations for HD 82943 (Fit 2) and GJ 876 (Keck and Lick Fit with $\sin i = 0.78$; see Table 2 in Laughlin & Chambers 2001), which can be viewed as genuine systems closest to the actual observations. Then, we generated 100 seed planets that all bear the same masses of Earth (where $M_\oplus \simeq 3.14 \times 10^{-3} M_{jup}$) in the simulations for each system. In Figure 8, we can see the distribution of the initial orbital elements for these postulated planets—they initially move on the less inclined belt with the relative inclination with regard to the plane of the resonant pair no more than 5° , the semi-major axis $a \in [0.96 \text{ AU}, 1.05 \text{ AU}]$, the eccentricity $e \in [0, 0.1]$, and the leftover arguments are set at random. Here we simply accounted for the near-circular orbits rather than much more eccentric orbits, because the life should develop and evolve in the biological environment without larger variations of temperature, implying the Earth-like planet should not move neither too close nor too far from the parent star.

For each star-two-planet-”Earth” four-body system, we carried out the integration for the timescale of 10^7 yr , to examine the dynamical habitability for the HD 82943 system.

As we shall see, we find that none of the orbits can be retained stable in the region at ~ 1 AU for the integration time, the seed planet travels on hyperbolic or parabolic orbits at the characteristic timescale $\tau < 2 \times 10^5$ yr (where 81% of them are ejected at $\tau \leq 5 \times 10^4$ yr and 95% at $\tau \leq 1.0 \times 10^5$ yr, see Figure 9a), owing to the scattering (Lin & Ida 1997) between two close resonant planets for the excitation in the eccentricity. A typical orbital evolution for the ejected orbits is shown in Figure 9b, the semi-major axis a grows from ~ 1 AU to over 100 AU, the eccentricity e undergoes a rapid increase from ~ 0.1 to 1 and the inclination i is also excited to a high value of $\sim 40^\circ$ (in some cases, the inclination can exceed 90°), finally, at 4,800 yr, the assumed Earth-like planet is scattered away from the two-planet system, while the orbital motions of the resonant planets remain as usual. The gravitational scattering on the terrestrial planet caused an unstable motion either as an ejection or a catastrophic collision with the star or planets due to the dynamical instabilities (Ford, Havlickova, & Rasio 2001). Our numerical investigations suggest that there will be at least a possibility for stable Earth-like orbits surviving in the range of [0.73 AU, 1.18 AU], even for wider habitable regions [0.75 AU, 1.40 AU] given by Kasting et al. (1993), which is in good agreement with the simulations by Menou & Tabachnik (2003). Analytically, Gladman (1993) attained the minimum separation Δ between two planets moving on initially circular orbits required for stability,

$$\Delta = 2\sqrt{3}R_H, \quad (14)$$

where the mutual Hill radius R_H is

$$R_H = \left(\frac{m_1 + m_2}{3m_0} \right)^{1/3} \left(\frac{a_1 + a_2}{2} \right). \quad (15)$$

For Fit 2, we achieve $\Delta \simeq 0.34$ AU and $R_H \simeq 0.10$ AU, which these values may become a bit different as the two planets for HD 82943 orbit on eccentric paths. Nevertheless, our goal here is to present a qualitative analysis, and we can easily notice that the initial orbits for the assumed planets are quite close to Hill sphere regime, resulting in their unstable motions. But it cannot rule out other stable regions for additional companions. For example, Sandquist et al. (2002) explored a three-planet case for HD 82943, which a supposed jovian planet with the mass of $0.5 M_{jup}$ at 0.02 AU was added to the system, and they found that this additional planet does not affect the orbital motion of the two outer planets and also not disturb the stability of this system. On the other hand, for the exterior domain extending to 30 AU \sim 50 AU or even farther out, does there exist the dust rings or circumstellar disk that are analogous to the Kuiper Belt being a remnant of the solar nebula? The recently launched SIRTf mission will provide fruitful information on this point in its ongoing tasks.

As a comparison, we accomplished the other same runs for GJ 876. And we conducted the four-body integrations for the time span of integration of 10^6 yr ($\sim 10^7$ orbital periods

for the innermost planet) and found all the systems are stable for the integration timescale. Figure 10 exhibits the typical orbital evolution for the Earth-like planet, both the semi-major axis a and the eccentricity e execute small fluctuations about 1 AU and 0.06, respectively, and the inclination i also remains less than 2 degrees in the same time span. And there is no sign to indicate that such regular orbits at ~ 1 AU with low eccentricities will become chaotic for much longer time even for the age of the star. Due to the faint luminosity for M4 star GJ 876, the habitable zones may reside in the range of [0.10 AU, 0.20 AU] (Kasting et al. 1993; Menou & Tabachnik 2003) sufficiently nearer to the orbits of GJ 876 b (~ 0.13 AU) and GJ 876 c (~ 0.21 AU) (Marcy et al. 2001; Laughlin & Chambers 2001; Rivera & Lissauer 2001), hence, the global chaos, corresponding to the circumstance of a collisional disruption or ejection, can always take place according to the Hill stability criterion (Gladman 1993; Chambers, Wetherill & Boss 1996) or direct numerical examinations, and exclude the possible existence of Earth-like planets for such habitable regions. Whereas Kuchner (2003) pointed out that a liquid planet with $a_p \geq 1.03$ AU $(L/L_\odot)^{1/2}$ (where for GJ 876, $a_p \geq 0.12$ AU) may exist under the protection of a thick steam atmosphere, it seems plausible for the Earth-like planets revolve around GJ 876 at the orbit about 1 AU, in the concept of the dynamical habitability. However, our predictions should be confirmed through careful investigation in future research if the Earth-like planets do survive secularly in such habitable zone. Firstly, the direct evidence of the presence for such planets strongly depend upon the future high resolution astrometric measurements, e.g., Space Interferometer Mission (SIM) or Terrestrial Planet Finder (TPF) that can provide much better precision than the present long-term precision of $\sim 2\text{-}3$ m s $^{-1}$ (Butler et al. 2003) for ground-based Doppler surveys. Secondly, the simulations of the runaway accretion of the planetary embryos (Laughlin et al. 2002) suggest that it is impossible for the Earth-mass planets to be formed in Habitable zones even for a well-separated system with near-circular orbits (e.g., 47 Uma), because the formation of the terrestrial planets are terrifically constrained by giant planet migration (Armitage 2003), therefore the depletion of small planetesimals in a disk-clearing phase may possibly take place when the massive planets sweep over them in their orbital decay process unless this orbital migration can halt at a proper position allowing for the continuous growth of the planetary embryos or the already-created Earth-like planets can also follow the migration with the giant planets in step and cease about the Habitable regions. Nevertheless, fortunately, the terrestrial planets are conceivable to survive in a modest fraction of systems where a single generation of massive planets formed (Armitage 2003) without significant migration.

5. The Possible Origin for the Orbital Geometry

The short-period giant planets that are close to the parent star with high temperature (e.g., 51 Peg, so-called hot Jupiter with $a < 0.1$ AU), are now thought to be formed through the shrinking orbital migration rather than be formed *in situ* due to the tidal interaction of a protoplanet with a surrounding gaseous disk (Ward 1997) and this orbital migration can originate from the exchange of angular momentum between the natal disk and protoplanet (Papaloizou 2003 and references therein). Now, it is widely believed that the migration will ubiquitously come about when two-planet systems suffer tidal interaction with an exterior disk, the outer planet will migrate inward until it gets trapped in a low order mean motion resonance with the inner companion (Bryden et al. 2000; Kley 2000) and the eccentricities will stop growing and be balanced as steady equilibrium values (Nelson & Papaloizou 2002) after being captured into the resonances.

For the aligned orbits of Type II, in the earlier works for GJ 876, Snellgrove et al. (2001) performed full hydrodynamical two-dimensional simulations to study the inward migration for GJ 876 planets interacting with each other and a protoplanetary disk, and the outer planet can be trapped into a 2:1 commensurability with the inner planet through slow migration, where the orbits were observed to be aligned with the resonant angles librating about zero (see also an overview in Papaloizou 2003) and the system can survive at least 2×10^7 orbits by the removal of the external disk. Subsequently, Lee & Peale (2002) showed that the forced inward migration of the outer companion of the GJ 876 system leads to certain capture into the observed resonances if the initial eccentricities are smaller enough where $e_1 \leq 0.06$ and $e_2 \leq 0.03$ with proper migration rates. They also revealed that after resonance capture, the eccentricities increase rapidly due to resonant interactions between the planets and the forced migration without eccentricity damping, while with parameterized eccentricity damping where $\dot{e}_i/e_i = -K|\dot{a}_i/a_i|$, the eccentricities can reach equilibrium values that remain unchanged for sufficiently long migration in the resonances. Recently, in the study of the evolution in resonant planetary systems (e.g., HD 82943), Kley et al. (2004) found that the two planets can enter into a 2:1 resonance in varying timescale provided that $e_2 < 0.25$, with both full hydrodynamical simulations and damped N-body calculations. They further suggested that there are several requirements for the 2:1 resonance capture—the more massive mass for the outer companion, the higher eccentricity of the inner planet and the apsidal alignment of $\theta_3 = 0^\circ$. In the case of Type II (Fit 2), where the eccentricity $e_2 = 0.18$ and a moderate $e_1 = 0.38$ and with two nearly equal planetary masses, or in the case of Fit 1b, where there can also be stable geometry about $e_2 \sim 0.25$ and a higher e_1 with a larger outer planet, in both cases the two planets undergo θ_3 -libration about 0° , thus we may comment that if the HD 82943 system is most likely to be aligned (Lee M.H. 2003, private communication), then the origin for such orbital geometry can be possibly attained by the

predictions of the hydrodynamic models (Kley et al. 2004), we will address this problem in our forthcoming paper.

For the antialigned orbits of Type III, Thommes & Lissauer (2003) argued that if the planets reached this configuration by migration in resonance, a significant mutual inclination between their orbits would seem to be required. As in this geometry, the two orbits for HD 82943 can experience the intersection on the co-orbital region (Ji et al. 2003c; Lee 2004), therefore a moderate inclination between two orbits can be achieved to act as a protection mechanism against close approaches (Thommes & Lissauer 2003). In §3.3.2, we also show that the highly inclined resonant configuration for this system can also be in presence, which the system is stabilized by both the 2:1 resonance and the apsidal phase-locking. However, for Fit 1a, although the HD 82943 system can be stable at least for 10^7 yr, it is still difficult to secure the resonant capture with N-body models due to the larger eccentricities of 0.41-0.54 in Kley et al. (2004), the origin for such configuration may attribute to an additional passing star’s influence or pure gravitational scattering mechanism (Lin & Ida 1997; Adams & Laughlin 2003), to pump up the eccentricities. One of the final fates in the scattering procedure is that the inner planet is left alone in the system with an eccentric orbit while the outer planet is ejected (Ford et al. 2001) into the stellar space, nearly immune to the gravitational influence from the parent star. If the scattering does happen in the course of the migration, a casual rapid capture may be required to prevent one of the planets from throwing away from the system and subsequently two orbits are well locked into 2:1 resonance (see §3.2.1) at larger eccentricities. Alternatively, another possible scenario is that both of the eccentricities are excited to moderate values when the 2:1 resonance is being crossed (Chiang et al. 2002), subsequently the continuous resonance crossings may terminate for the suitable eccentricities evolved into the resonance geometry.

6. Summary and Remarks

In this paper, we have explored the stable geometry for a system with two planets involved in a 2:1 MMR, and we mainly concentrate on the study of the HD 82943 system by adopting two different sets of the orbital parameters. In our numerical simulations, we found there are three possible stable configurations for HD 82943 system:(1)Type I, only $\theta_1 \approx 0^\circ$, (2)Type II, $\theta_1 \approx \theta_2 \approx \theta_3 \approx 0^\circ$ (aligned case), and (3)Type III, $\theta_1 \approx 180^\circ$, $\theta_2 \approx 0^\circ$, $\theta_3 \approx 180^\circ$ (antialigned case). The direct integrations show that all stable orbits are related to the 2:1 commensurability that remains the semi-major axes for two companions slightly vary about the initial values over the secular dynamical evolution for 10^7 yr, further the apsidal phase-locking for two planets can enhance the stability for this system, because the eccentricities are

simultaneously preserved to prevent the planets from frequent close encounters. Additionally, we comment that other systems trapped in 2:1 MMR (e.g. GJ 876 or possibly HD 160691) can select one of the aforementioned three stable topology in their authentic orbital motions, which are determined by their initial parameters. And we underline that such configurations, making up the dynamical families, can serve as a general regulation for the long-term stable orbits of the 2:1 resonant exosystems. In final, we summarize some conclusions:

Using the earlier best-solutions of Fit 1, we found three types of stable orbits for HD 82943, while we observed the steady configurations of Types I and II by employing the new solution of Fit 2 supplied by Mayor et al. (2004). In the meantime, we also proposed a semi-analytical model to study the $e_i - \Delta\varpi$ Hamiltonian contour determined by the initial parameters, and the closest level curves encompass the direct numerical results, which presents a good agreement between them. The theoretical figures can still provide valuable information on the dynamics for two planets.

Given the stable geometry based on Fit 2, we then extensively examined the dependence of the stability of HD 82943 in the orbital parameter space and the planetary mass ratios. In the case of the non-coplanar circumstances, we found that stability requires that the relative inclination be $\sim 25^\circ$ or less. For a fixed planetary mass ratio ~ 1 , the stable orbits for HD 82943 requires $\sin i \geq 0.50$. For the non-constant mass ratio case (where m_2 is kept), the requirement of the stability is $m_1/m_2 \leq 2$, which indicates an upper boundary for the mass of the inner planet. Concerning the eccentricities, the system can be always steady when $0 < e_2 \leq 0.24$ and $0 < e_1 < 0.60$. In a word, these outcomes do demonstrate that the stability for HD 82943 is strongly sensitive to the sound planetary masses, rather lower relative inclination between two orbits, the eccentricities and other orbital parameters. In addition, we showed that the assumed terrestrial bodies cannot exist in the habitable zones of HD 82943 thanks to strong perturbations induced by two massive planets, but the Earth-like planets can be dynamically habitable in the GJ 876 system at ~ 1 AU in the numerical surveys.

However, as the additional measurements will improve the present best-fit solution for HD 82943 with a corrected model by taking into account the planet-planet interactions. Thus, we hope to have more precise orbital solution not only to check for our presented predictions in this paper but to better make sense of the complete dynamics and the origin of this system in the near future.

We thank G. Laughlin, M.H. Lee, S.J. Peale, J.C.B. Papaloizou and E. Thommes for informative discussions and helpful explanations, K. Gozdziewski for good comments. We are grateful to M. Mayor and S. Udry for providing us their manuscript. We also thank E. Bois

for sending us his unpublished figures. This work is financially supported by National Natural Science Foundation of China (Grants No.10203005, 10173006, 10233020) and Foundation of Minor Planets of Purple Mountain Observatory. This research has made use of NASA's Astrophysics Data System (ADS).

REFERENCES

- Adams, F., & Laughlin, G. 2003, *Icarus*, 163, 290
- Armitage, P. J. 2003. *ApJ*, 582, L47
- Barnes, R., & Quinn, T. 2004, *ApJ*, submitted, (astro-ph/0401171)
- Beauge, C., Ferraz-Mello, S., & Michtchenko, T.A. 2003, *ApJ*, 593, 1124
- Beauge, C., & Michtchenko, T.A. 2003, *MNRAS*, 341, 760
- Bois, E., et al. 2003, *ApJ*, 598, 1312
- Brouwer, D., & Clemence, G. M. 1961, *Methods of Celestial Mechanics* (New York: Academic)
- Bryden, G., et al. 2000, *ApJ*, 540, 1091
- Butler, R. P., et al. 2003, *ApJ*, 582, 455
- Callegari Jr., N., Michtchenko, T.A., & Ferraz-Mello, S. 2004, *Cel. Mech. & Dyn. Astron.*, 89, in press
- Chambers, J. E., Wetherill, G. W., & Boss, A. 1996, *Icarus*, 119, 261
- Chiang, E.I., Tabachnik, S., & Tremaine, S. 2001, *AJ*, 122, 1607
- Chiang, E.I., Fischer, D., & Thommes, E. 2002, *ApJ*, 564, L105
- Chiang, E.I. 2003, *ApJ*, 584, 465
- Cohen, C.J., & Hubbard, E.C. 1965, *AJ*, 70, 10
- Duncan, M.J., Levison, H.F., & Budd, S.M. 1995, *AJ*, 110, 3073
- Dvorak, R., et al. 2003, *A&A*, 410, L13
- Feng K. 1986, *J. Comp. Math.*, 4, 279
- Ferraz-Mello, S., Beauge, C., & Michtchenko, T. 2003, *Cel. Mech. & Dyn. Astron.*, 87, 99
- Fischer, D., et al. 2001, *ApJ*, 551, 1107
- Fischer, D., et al. 2003, *ApJ*, 586, 1394

- Fischer, D. A., Valenti, J., & Marcy, G. 2004, in ASP Conf. Ser., S219, Stars as Suns: Activity, Evolution and Planets, ed. A. Dupree and A. Benz, (San Francisco: ASP), in press
- Ford, E. B., Rasio, F. A., & Sills, A. 1999, *ApJ*, 514, 411
- Ford, E. B., Havlickova, M., & Rasio, F. A. 2001, *Icarus*, 150, 303
- Gladman, B. 1993, *Icarus*, 106, 247
- Goldreich, P., & Tremaine, S. 1980, *ApJ*, 241, 425
- Gozdziewski, K., & Maciejewski, A.J. 2001, *ApJ*, 563, L81
- Gozdziewski, K. 2003, *A&A*, 398, 1151
- Gozdziewski, K., & Maciejewski, A.J. 2003, *ApJ*, 586, L153
- Gozdziewski, K., Konacki, M., & Maciejewski, A.J. 2003, *ApJ*, 594, 1019
- Gould, A., Ford, E. B., & Fischer, D.A. 2003, *ApJ*, 591, L155
- Hadjidemetriou, D.H. 2002, *Cel. Mech. & Dyn. Astron.*, 83, 141
- Hadjidemetriou, D.H., & Psychoyos D. 2003, *Lecture Notes in Physics*, accepted
- Haghighipour, N., et al. 2003, *ApJ*, 596, 1332
- Israelian, G., et al. 2001, *Nature*, 411, 163
- Israelian, G., et al. 2003, *A&A*, 405, 753
- Jiang, I.G., & Yeh, L.C. 2004, *AJ*, submitted
- Ji, J. H., Li, G.Y., & Liu, L. 2002, *ApJ*, 572, 1041
- Ji, J. H., et al. 2003a, *ApJ*, 585, L139
- Ji, J. H., et al. 2003b, *ApJ*, 591, L57
- Ji, J. H., et al. 2003c, *Cel. Mech. & Dyn. Astron.*, 87, 113
- Jones, B., & Sleep, P. 2002, *A&A*, 393, 1015
- Jones, H.R.A., et al. 2002, *MNRAS*, 337, 1170
- Kasting, J. F., Whitmore, D. P., & Reynolds, R. T. 1993, *Icarus*, 101, 108

- Kinoshita, H. & Nakai, H. 2001, PASJ, 53, L25
- Kinoshita, H., & Nakai, H. 1985, *Cel. Mech.*, 36, 391
- Kinoshita, H., & Nakai, H. 2000, in ASP Conf. Ser., S202, *Planetary Systems in the Universe*, ed. A. J. Penny, P. Artymowicz, A. -M. Lagrange, and S. S. Russell (San Francisco: ASP), in press
- Kinoshita, H., & Nakai, H. 2002, in Proc. 34rd Symp. Celest. Mech., in press
- Kiseleva-Eggleton, L., et al. 2002, *ApJ*, 578, L145
- Kley, W. 2000, *MNRAS*, 313, L47
- Kley, W. 2003, *Cel. Mech. & Dyn. Astron.*, 87, 85
- Kley, W., Peitz, J., & Bryden, G. 2004, *A&A*, 414, 735
- Kuchner, M.J. 2003, *ApJ*, 596, L105
- Laughlin, G., & Chambers, J. 2001, *ApJ*, 551, L109
- Laughlin, G., Chambers, J., & Fischer, D. 2002, *ApJ*, 579, 455
- Lee, M.H., & Peale, S.J. 2002, *ApJ*, 567, 596
- Lee, M.H., & Peale, S.J. 2003, *ApJ*, 592, 1201
- Lee, M.H. 2004, *ApJ*, submitted, (astro-ph/0401410)
- Lin, D. N. C., Bodenheimer, P., & Richardson, D. C. 1996, *Nature*, 380, 606
- Lin, D. N. C., & Ida, S. 1997, *ApJ*, 477, 781
- Lissauer, J. J., & Rivera, E. J. 2001, *ApJ*, 554, 1141
- Menou, K., & Tabachnik, S. 2003, *ApJ*, 583, 473
- Malhotra, R. 2002, *ApJ*, 575, L33
- Mazeh, T., & Zucker, S. 2003, *ApJ*, 590, L115
- Marcy, G.W., Cochran, W. D. & Mayor, M. 2000, in *Protostars and Planets IV*, ed. V. Mannings, A.P. Boss & S. S. Russell (Tucson: University of Arizona Press), p.1285
- Marcy, G. W., et al. 2001, *ApJ*, 556, 296

- Marcy, G.W., et al. 2003, in *Scientific Frontiers in Research on Extrasolar Planets*, ed. D. Deming and S. Seager (Washington DC: ASP), Vol.294, p.1
- Mayor, M., & Queloz D. 1995, *Nature*, 378, 355
- Mayor, M., et al. 2004, *A&A*, 415, 391
- Murray, C. D., & Dermott, S. F. 1999, *Solar System Dynamics* (New York: Cambridge Univ. Press).
- Murray, N., Paskowitz, M., & Holman, M. 2002, *ApJ*, 565,608
- Naef, D., et al. 2001, *A&A*, 375, L27
- Nelson, R. P., Papaloizou, J.C.B., Masset,F. , & Kley, W. 2000, *MNRAS*, 318, 18
- Nelson, R.P., & Papaloizou,J.C.B. 2002, *MNRAS*, 333, L26
- Papaloizou, J.C.B. 2003, *Cel. Mech. & Dyn. Astron.*, 87, 53
- Peale,S.J. 2003, *Cel. Mech. & Dyn. Astron.*, 87, 129
- Rivera, E. J., & Lissauer, J. J. 2000, *ApJ*, 530, 454
- Rivera, E. J., & Lissauer, J. J. 2001, *ApJ*, 558, 392
- Santos, N., Israelian, G., & Mayor, M. 2001, *A&A*, 373, 1019
- Santos, N., et al. 2003, *A&A*, 398, 363
- Sandquist, E.L., et al. 2002 ,*ApJ*, 572,1012
- Snellgrove, M.D., Papaloizou, J.C.B., & R. P., Nelson. 2001, *A&A*, 374, 1092
- Thommes, E., & Lissauer, J. J. 2003,*ApJ*, 597, 566
- Wan, X. S., & Huang, T. Y. 2001, *A&A*, 368, 700
- Ward, W. R. 1997, *Icarus*, 126, 261
- Weidenschilling, S. J., & Marzari, F. 1996, *Nature*, 384, 619
- Wisdom, J., & Holman, M. 1991, *AJ*,102,1528
- Zhou, L. Y., et al. 2004, *MNRAS*, submitted,(astro-ph/0310121)
- Zhou, J. L., & Sun Y. S. 2003, *ApJ*, 598, 1290

A. The form of the total angular momentum with use of Jacobi coordinates

The Hamiltonian with use of Jacobi coordinates has the following form:

$$F = \frac{1}{2}\sigma_1\dot{\mathbf{r}}_1^2 + \frac{1}{2}\sigma_2\dot{\mathbf{r}}_2^2 - \frac{Gm_0m_1}{r_{01}} - \frac{Gm_0m_2}{r_{02}} - \frac{Gm_1m_2}{r_{12}}, \quad (\text{A1})$$

where

$$\sigma_1 = \frac{m_0m_1}{m_0 + m_1}, \sigma_2 = \frac{m_2(m_0 + m_1)}{m_0 + m_1 + m_2}. \quad (\text{A2})$$

Now we have two choices for the unperturbed Hamiltonian:

A)

$$F_0 = \frac{1}{2}\sigma_1\dot{\mathbf{r}}_1^2 - \frac{Gm_0m_1}{r_1} + \frac{1}{2}\sigma_2\dot{\mathbf{r}}_2^2 - \frac{Gm_0m_2}{r_2} \quad (\text{A3})$$

B)

$$F_0 = \frac{1}{2}\sigma_1\dot{\mathbf{r}}_1^2 - \frac{Gm_0m_1}{r_1} + \frac{1}{2}\sigma_2\dot{\mathbf{r}}_2^2 - \frac{Gm_2(m_0 + m_1)}{r_2}. \quad (\text{A4})$$

The difference between A) and B) is the last term. The choice A) is recently popular. In the treatment of the triple star system the choice B) is always adopted, since the form of the disturbing function becomes simpler for the case $r_1 < r_2$.

The unperturbed Hamiltonian takes the following form for each case:

A)

$$F_0 = -\frac{Gm_0m_1}{2a_1} - \frac{Gm_0m_2}{2a_2}, \quad (\text{A5})$$

B)

$$F_0 = -\frac{Gm_0m_1}{2a_1} - \frac{G(m_0 + m_1)m_2}{2a_2}. \quad (\text{A6})$$

The form of the total angular momentum J is

A)

$$\sigma_1\sqrt{G(m_0 + m_1)a_1(1 - e_1^2)} + \sigma_2\sqrt{Gm_0\frac{m_0 + m_1 + m_2}{m_0 + m_1}a_2(1 - e_2^2)}, \quad (\text{A7})$$

B)

$$\sigma_1\sqrt{G(m_0 + m_1)a_1(1 - e_1^2)} + \sigma_2\sqrt{G(m_0 + m_1 + m_2)a_2(1 - e_2^2)}. \quad (\text{A8})$$

In the above expressions the meaning of the osculating elements a_2, e_2 is different between A) and B), because the unperturbed form is different. However, for the averaged Hamiltonian after the elimination of the short periodic terms, the difference due to the choice between the Jacobi coordinates and heliocentric (or astrometric) coordinates is the order of the perturbation $(m_1/m_0, m_2/m_0)$, which could be negligible.

Table 1. The orbital parameters of HD 82943 planetary system (Fit 1^a). $m_0 = 1.05M_\odot$

| Parameter | Fit 1a | | Fit 1b | |
|----------------------|-----------|-----------|-----------|-----------|
| | Outer (b) | Inner (c) | Outer (b) | Inner (c) |
| $m \sin i (M_{Jup})$ | 1.63 | 0.88 | 1.63 | 0.88 |
| $P(\text{days})$ | 444.6 | 221.6 | 444.6 | 221.6 |
| $a(\text{AU})$ | 1.16 | 0.73 | 1.16 | 0.73 |
| e | 0.41 | 0.54 | 0.41 | 0.54 |
| $\Omega(\text{deg})$ | 14.79 | 154.23 | 327.65 | 239.11 |
| $\omega(\text{deg})$ | 96.0 | 138.0 | 96.0 | 138.0 |
| Mean Anomaly(deg) | 97.86 | 10.02 | 53.40 | 188.50 |

^aThe orbital parameters for the planetary masses, orbital periods, semi-major axes, eccentricities and apsidal arguments are taken from the Geneva website, as of July 31, 2002. Both of the inclinations are assumed to be 0.5° . Note Fit 1a and Fit 1b are, respective, one of Types III and II, amongst 100 first runs.

Table 2. The orbital parameters of HD 82943 planetary system (Fit 2^a). $m_0 = 1.15M_\odot$

| Parameter | Outer (b) | Inner (c) |
|----------------------|-----------|-----------|
| $m \sin i (M_{Jup})$ | 1.84 | 1.85 |
| $P(\text{days})$ | 435.1 | 219.4 |
| $a(\text{AU})$ | 1.18 | 0.75 |
| e | 0.18 | 0.38 |
| $\Omega(\text{deg})$ | 120.91 | 315.60 |
| $\omega(\text{deg})$ | 237.0 | 124.0 |
| Mean Anomaly(deg) | 168.56 | 185.12 |

^aThe orbital parameters for the planetary masses, orbital periods, semi-major axes, eccentricities and the periastron arguments are adopted from Mayor et al. (2004), as of October 13, 2003. The inclinations are the same as given in Table 1. The mean anomalies are derived at the epoch JD 2,452,396.82. Fit 2 is one of Type II of 100 second runs.

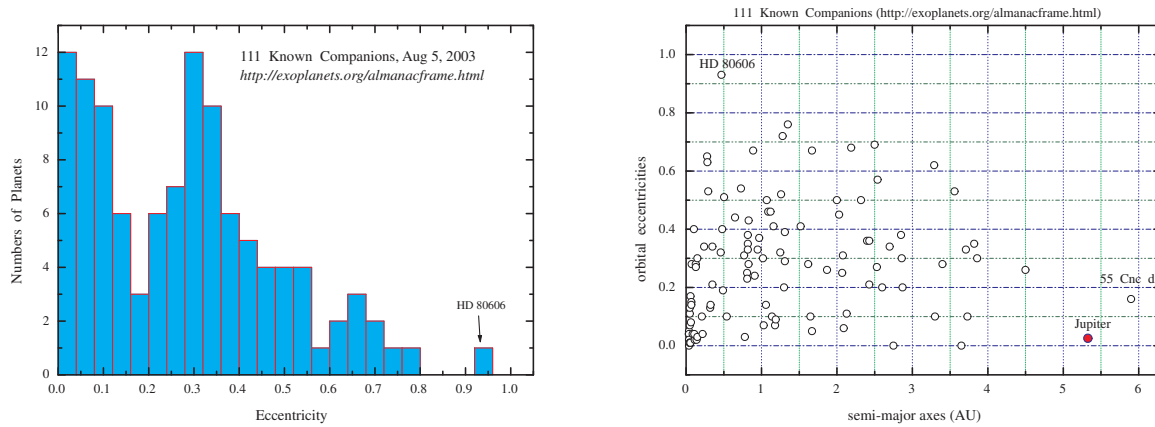


Fig. 1.— *Left panel:* the histogram for the eccentricities for 111 extrasolar planets, as of Aug. 5, 2003. Notice that over 50% of the planets have the eccentricities larger than 0.30, and HD 80606 b can occupy the eccentricity up to 0.93. *Right panel:* distribution of the semi-major axes plotted against the eccentricities. Note that 55 Cnc d can be distant as far as nearly 6 AU (see also Marcy et al. 2003) from its parent star.

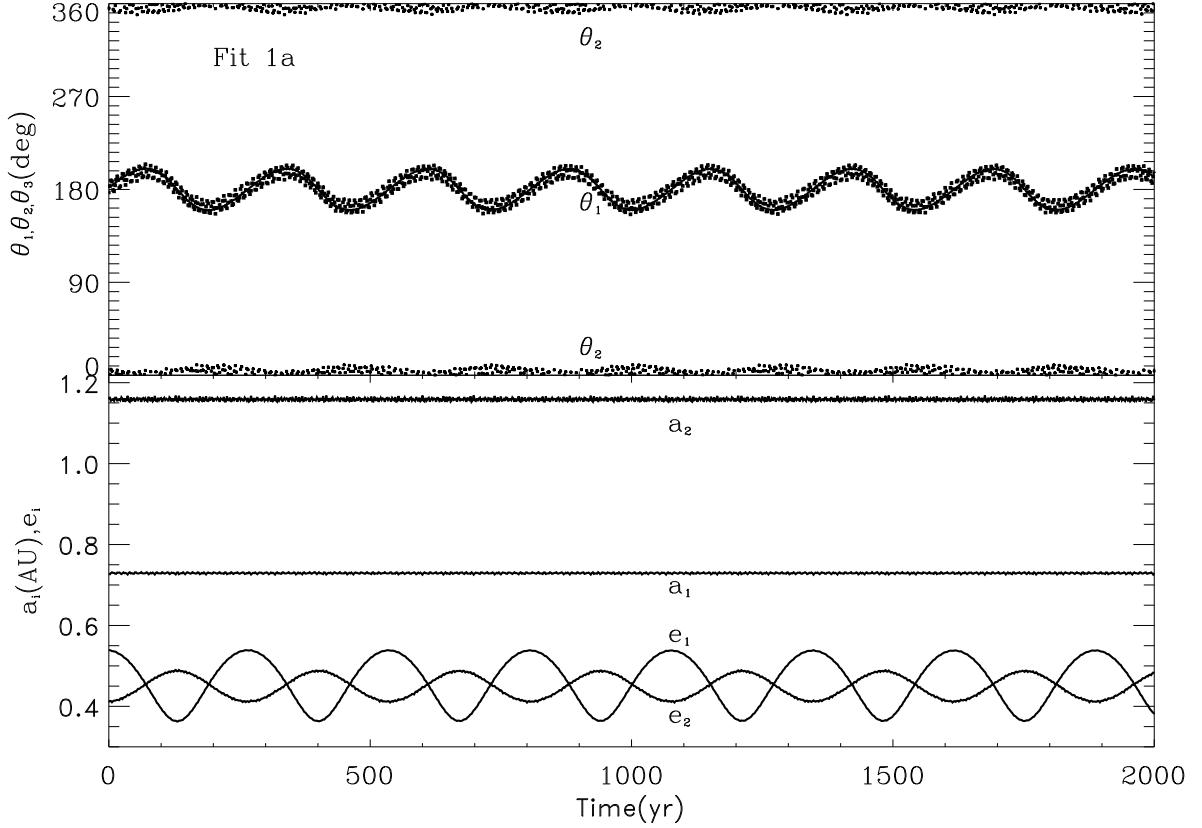


Fig. 2.— Orbital evolution for Fit 1a (antialigned orbits). *Upper panel:* θ_1 librates (by *dots*) about 180° with a moderate amplitude of $\sim 30^\circ$, θ_2 (by *dots*) about 0° with a small amplitude of $\sim 10^\circ$, and θ_3 (by *thick line*) about 180° with a relatively small amplitude of $\sim 30^\circ$ for $t = 10^7$ yr (to see more clearly, we simply display a snapshot for $t = 2000$ yr). *Lower panel:* a_1 and a_2 slightly vibrate about 0.73 and 1.15 AU for $t = 10^7$ yr. Notice that e_1 and e_2 separately reside in (0.36, 0.56) and (0.39, 0.49). The 2:1 resonance is confirmed by the modulations of the semi-major axes a_i and θ_i ($i = 1, 2$). Note that θ_1 and θ_3 share the same libration period of ~ 300 yr.

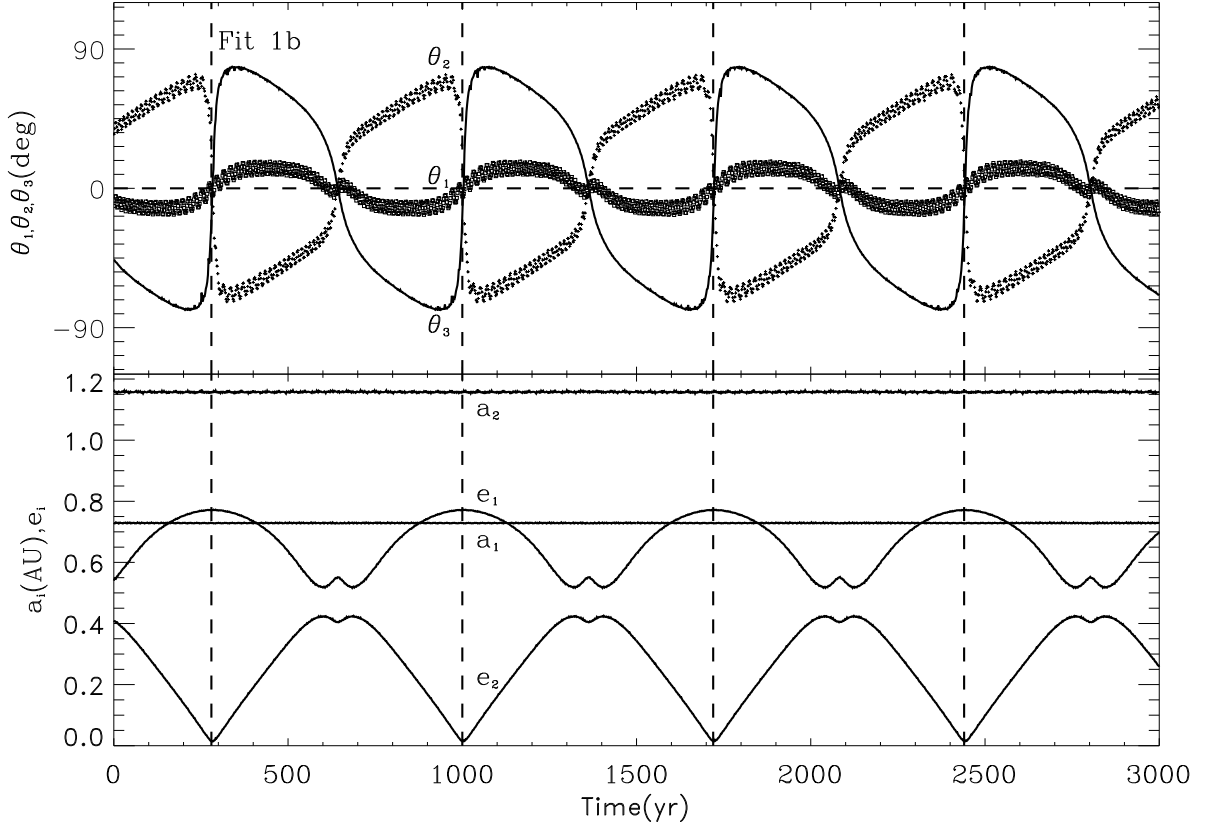


Fig. 3.— Orbital evolution for Fit 1b (aligned orbits). *Upper panel:* θ_1 (by *square sign*) librates about 0° with a small amplitude of $\sim 20^\circ$, but θ_2 (by *plus sign*) and θ_3 (by *thick line*) individually librate about 0° (a snapshot for $t = 3000$ yr) with a large amplitude of $\sim 70^\circ$. In this resonant aligned geometry, we again observe that θ_1 , θ_2 and θ_3 share the common librating periods of ~ 700 yr, coupled with those of the eccentricities of e_1 and e_2 . *Lower panel:* a_1 and a_2 do not change dramatically but undergo small oscillations about 0.73 AU and 1.15 AU for $t = 10^7$ yr, further the eccentricities e_1 and e_2 librate in the range of (0.5, 0.8) and (0, 0.45), respectively, in the behavior of the converse cycles, owing to the conservation of the total angular momenta for the system.

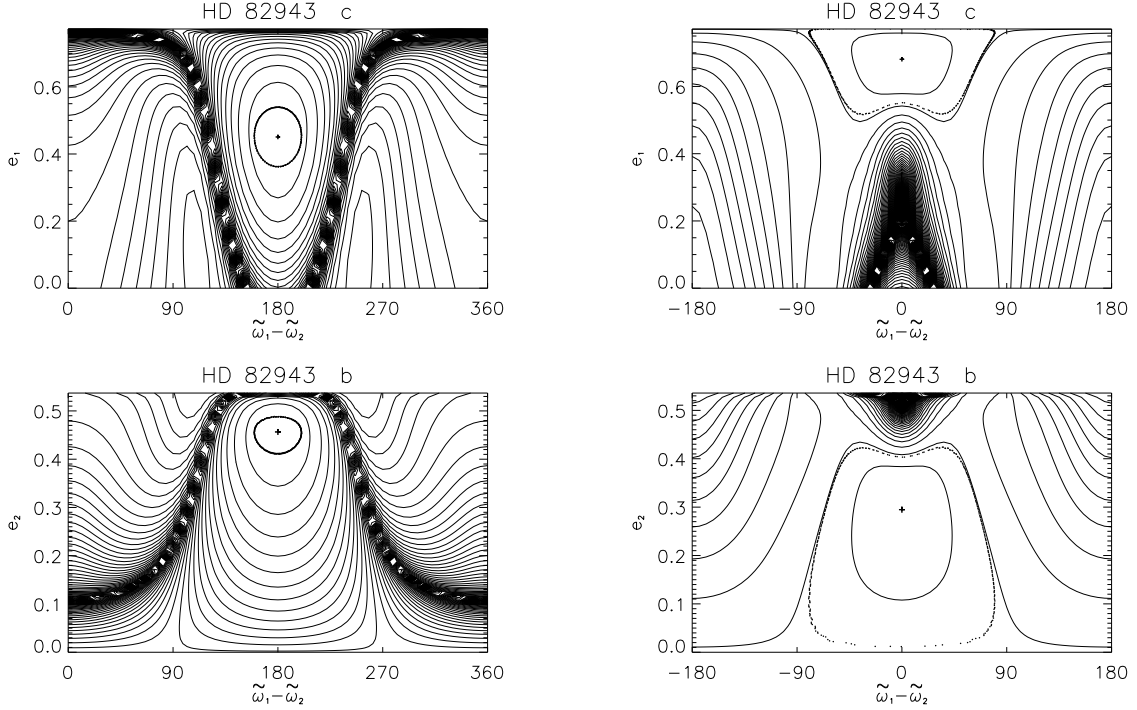


Fig. 4.— e - $\Delta\varpi$ Hamiltonian contour map for Fit 1. *Left panel:* (a) For Fit 1a, the contour levels are exhibited by *thin line* and the numerical solutions shown by *thick line* (the innermost curve about plus). The marked *plus* denotes the stationary solutions – $(180^\circ, 0.45)$ and $(180^\circ, 0.46)$, respectively. *Right panel:* (b) For Fit 1b, *thin line* for contour levels and *dotted points* for numerical solutions, the librating centers are, respectively, $(0^\circ, 0.68)$ and $(0^\circ, 0.29)$. The $e_i - \Delta\varpi$ figures both show a good agreement between the numerical results and the semi-analytical solutions.

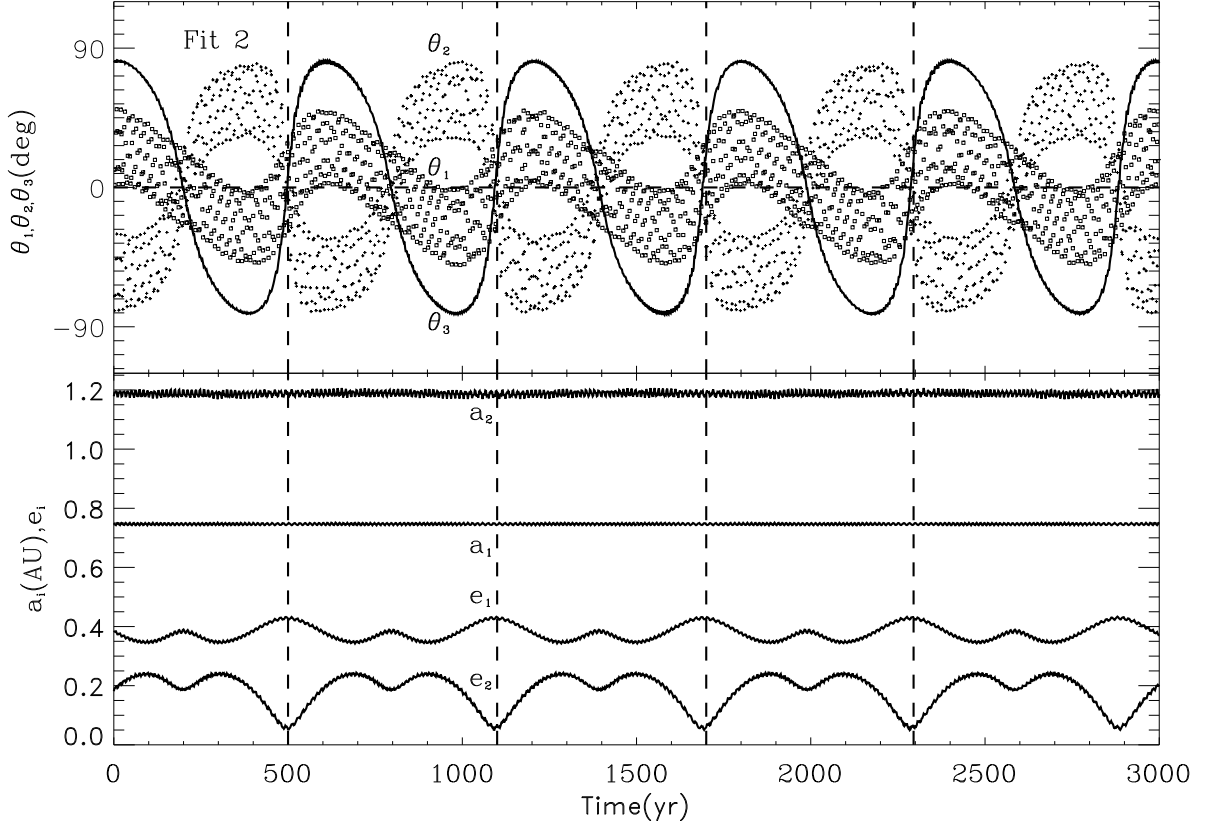


Fig. 5.— Orbital variations for Fit 2 (aligned orbits). *Upper panel:* θ_1 (by *square sign*) librates about 0° with a moderate amplitude of $\sim 45^\circ$, but θ_2 (by *plus sign*) and θ_3 (by *thick line*) individually librate about 0° (a snapshot for $t = 3000$ yr) with large amplitude of $\sim 80^\circ$. *Lower panel:* the semi-major axes a_1 and a_2 are almost unchanged and they modulate about 0.75 AU and 1.18 AU with relatively smaller amplitude for $t = 10^7$ yr, at this time, the amplitude of the oscillations for e_1 and e_2 are not so large and they are just wandering in the span (0.34, 0.44) and (0, 0.25), respectively. Notice that the eccentricities have the libration periods of ~ 600 yr, which are coupled with those of θ_1 and θ_3 .

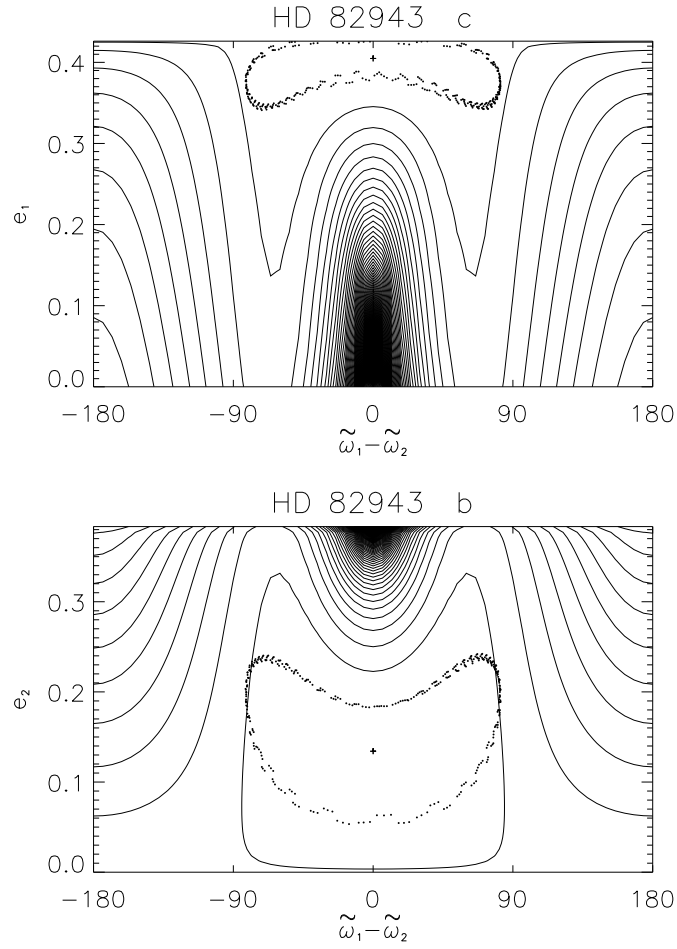


Fig. 6.— $e-\Delta\varpi$ Hamiltonian contour map for Fit 2. Same as the definition in Figure 4b. The equilibrium points are: $(0^\circ, 0.40)$ and $(0^\circ, 0.13)$, respectively.

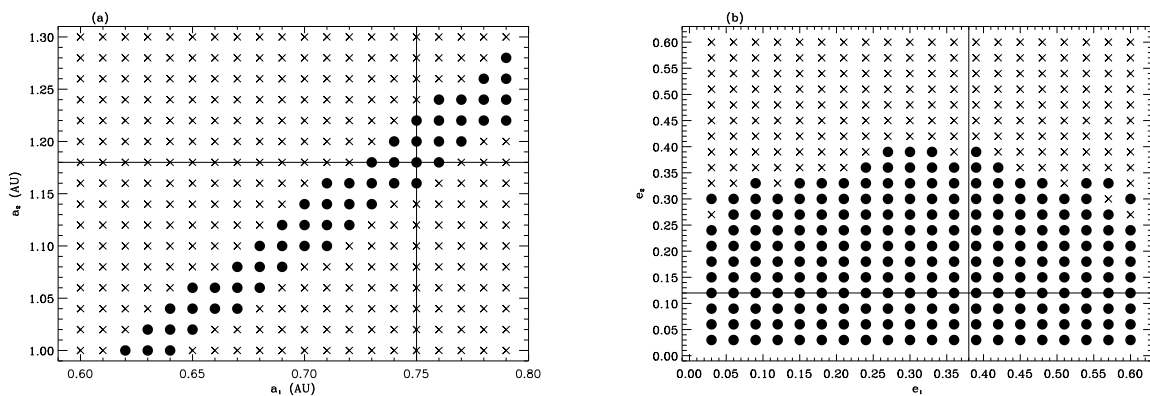


Fig. 7a-7b.— (a-b)The stable maps in the parameter spaces of $[a_1, a_2]$ and $[e_1, e_2]$. (c-d)The stable maps in the parameter spaces of $[M_1, M_2]$ and $[\omega_1, \omega_2]$. The sign *crosses* indicate the unstable orbits and *filled circles* for stable orbits lasting for 10^6 yr. The intersection between the vertical and horizontal lines represents for the present solution from Fit 2.

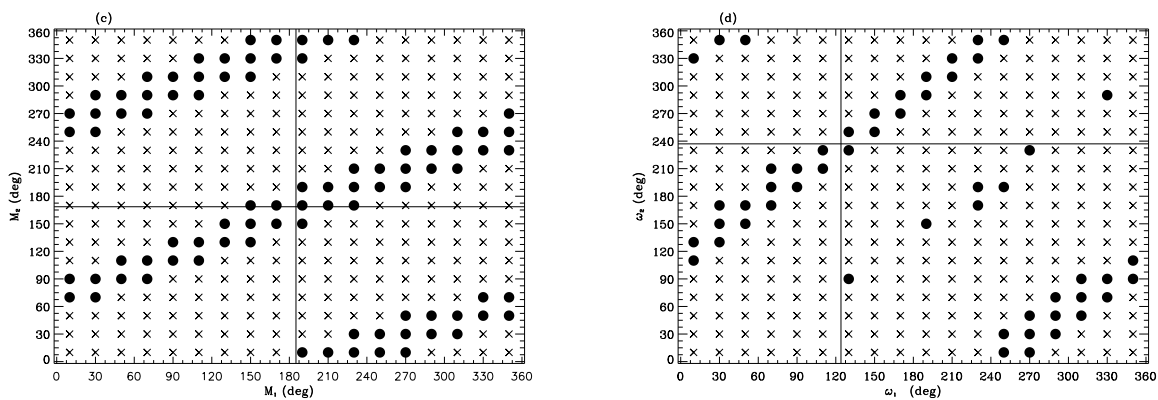


Fig. 7c-7d.—

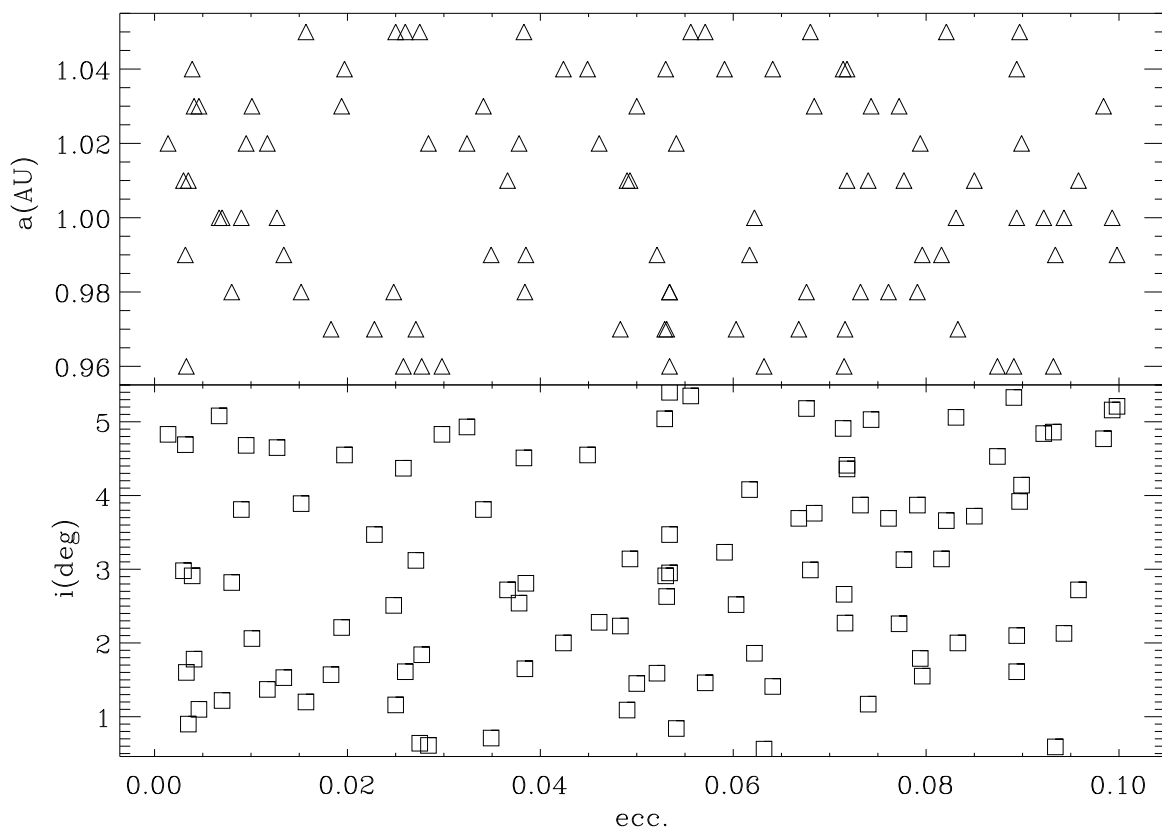


Fig. 8.— Initial orbital parameters for 100 seed Earth-like planets. *Upper panel*: the distribution of $[e, a]$, where $a \in [0.96\text{AU}, 1.05\text{AU}]$ with the incremental step of 0.01 AU, and $e \in [0, 0.1]$, indicating the initial near-circular orbits for testing the dynamical habitability. *Lower panel*: eccentricity versus inclination, where $i \in [0^\circ, 5^\circ]$, showing that these seed planets are almost in the same plane with the resonant pairs.

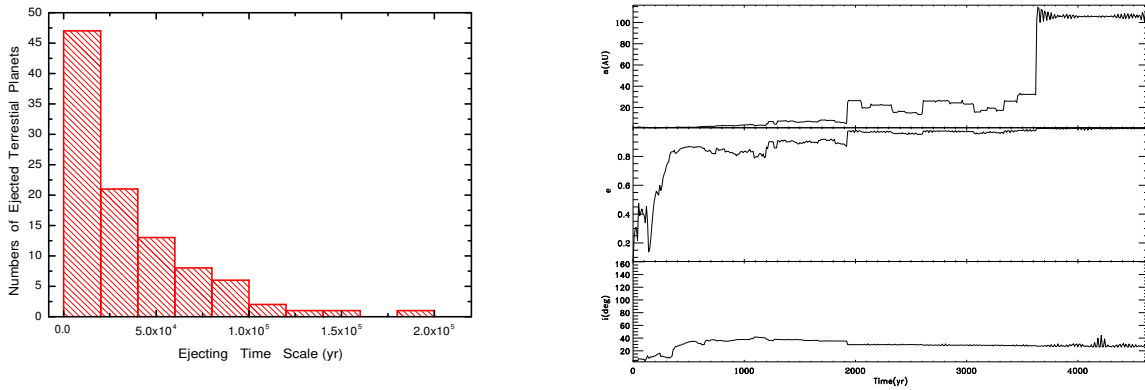


Fig. 9.— *Left panel:* (a) The numbers of the ejected terrestrial planet vs ejecting timescale. Notice that 95% of the orbits are ejected at $\tau \leq 1.0 \times 10^5$ yr. *Right panel:* (b) A typical orbital evolution for the ejected orbits in the HD 82943 system: the semi-major axis a grows from ~ 1 AU to over 100 AU, the eccentricity e undergoes a rapid increase from ~ 0.1 to 1 and the inclination i is also excited to a high value of $\sim 40^\circ$. Finally, the assumed Earth-like planet is ejected away from the two-planet system at 4,800 yr.

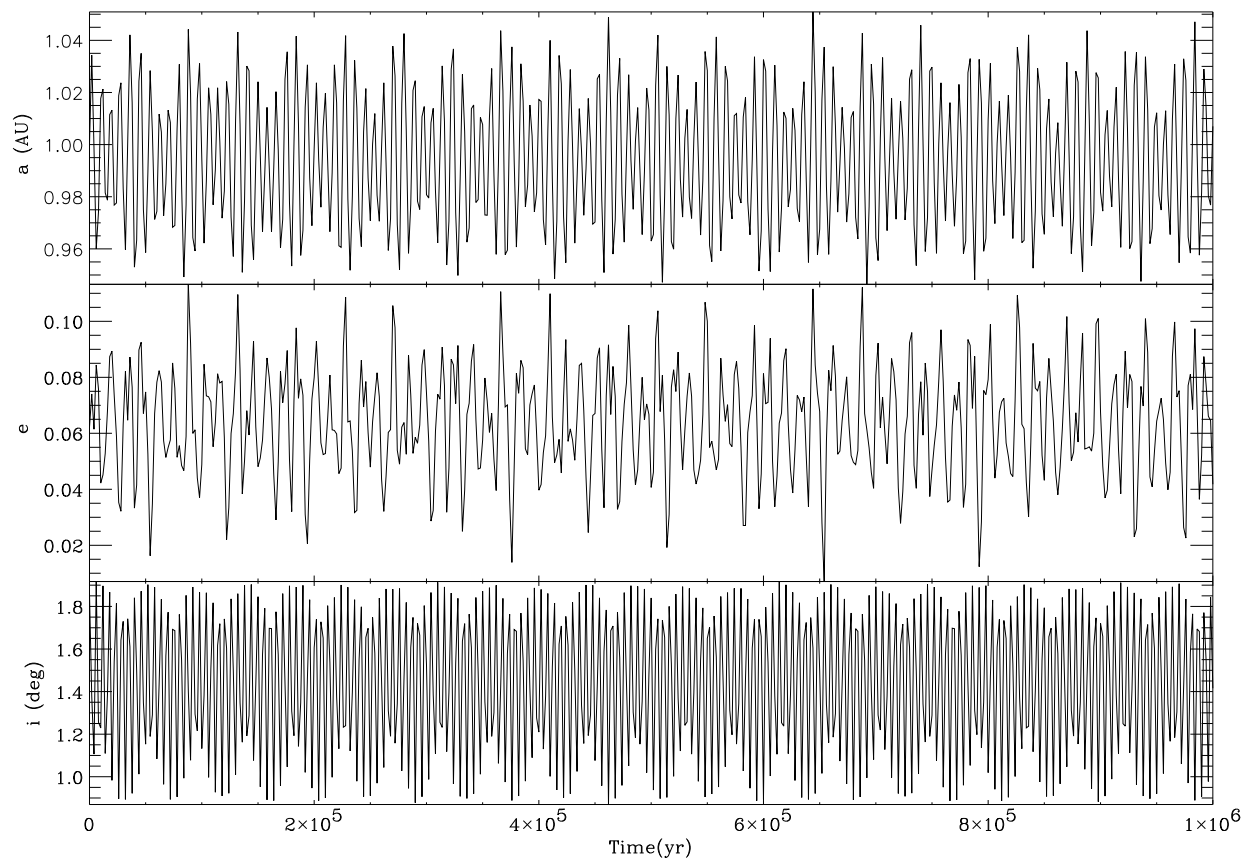


Fig. 10.— Orbital variations for possible Earth-like planet in the GJ 876 system. Both the semi-major axis a and the eccentricity e execute small fluctuations about 1 AU and 0.06, respectively, and the inclination i also remains less than 2 degrees over the same time span. And there is no sign to indicate that such regular orbits at ~ 1 AU with lower eccentricities will become chaotic for much longer time, even for the age of the star.